LA-7114-TR
Translation

High-Energy, Twelve-Channel Laser Facility (DELFIN) for Spherical Irradiation of Thermonuclear Targets

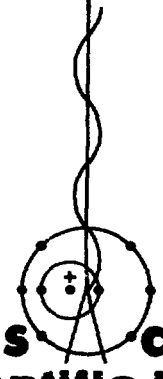

los alamos
scientific laboratory
of the University of California
LOS ALAMOS, NEW MEXICO 87545

An Affirmative Action/Equal Opportunity Employer

UNITED STATES
DEPARTMENT OF ENERGY
CONTRACT W-7405-ENG. 36

LA-7114-TR
Translation
UC-21
Issued: March 1978

los alamos
scientific laboratory
of the University of California
LOS ALAMOS, NEW MEXICO 87545

High-Energy, Twelve-Channel Laser Facility (DELFIN) for Spherical Irradiation of Thermonuclear Targets

by

N. G. Basov, A. E. Danilov, O. N. Krokhin, B. V. Kruglov, Yu. A. Mikhailov, G. V. Sklizkov, S. I. Fedotov, and A. N. Fedorov

USSR Academy of Sciences
P. N. Lebedev Physics Institute

Preprint Number 74

Translated by I. O. Bohachevsky

HIGH-ENERGY, TWELVE-CHANNEL LASER FACILITY (DELFIN) FOR SPHERICAL IRRADIATION OF THERMONUCLEAR TARGETS

by

N. G. Basov, A. E. Danilov, O. N. Krokhin, B. V. Kruglov, Yu. A. Mikhailov, G. V. Sklizkov, S. I. Fedotov, and A. N. Fedorov

USSR Academy of Sciences
P. N. Lebedev Physics Institute

Preprint Number 74

Translated by I. O. Bohachevsky

ABSTRACT

This paper describes a high-energy, twelve-channel laser facility (DELFIN) intended for high-temperature heating of thermonuclear targets with spherical symmetry. The facility includes a neodymium-glass laser with the ultimate radiation energy of 10 kJ, a pulse length of approximately 10^{-10} to 10^{-9} s, beam divergence of 5×10^{-4} radians, a vacuum chamber in which laser radiation interacts with the plasma, and a system of diagnostic instrumentation for the observation of laser beam and plasma parameters. Described are the optical scheme and construction details of the laser facility. Presented is an analysis of focusing schemes for target irradiation and described is the focusing scheme of the DELFIN facility, which is capable of attaining a high degree of spherical symmetry in irradiating targets with maximum beam intensity at the target surface of approximately 10^{15} W/cm^2. This paper examines the most important problems connected with the physical investigations of thermonuclear laser plasma and the basic diagnostic problems involved in their solution.

NOMENCLATURE

LTS	-	Laser-initiated (controlled) thermonuclear fusion
VKU	-	Final amplification stage
E_L	-	Final laser energy
ZG	-	Pulse generator
K	-	Amplification coefficient for the stage
K_E	-	Contrast coefficient for radiation
LPKU	-	Linear preamplification stage
MKU	-	High-energy amplification stage
MLU	-	High-energy laser facility
PKU	-	Preamplification stage
RLP	-	Laser-triggered spark gap
SP	-	Component beam
UV	-	Shock wave
EOP	-	Electro-optical transformer
B	-	Brightness
$\Delta\tau$	-	Time separation of different beams
n	-	Beam splitting coefficient
n_e	-	Electron density
q	-	Energy density in the beam
S	-	(Rear apical interval) Focal length
YAG	-	Yttrium-aluminum garnet
α	-	Beam divergence
E	-	Specific plasma energy
E_{pr}	-	Beam stability in the glass
μ	-	Fill coefficient for area of the target
Ω	-	Overall solid angle of convergence of laser radiation on target.

During the past number of years[1] in laser-controlled thermonuclear fusion research, significant attention was devoted to the construction of powerful laser systems for spherically symmetric irradiation of plasma[2-8] and to the diagnostic instrumentation for the study of its parameters.[9-16] Analysis of different laser-fusion concepts[17-26] indicates that for the achievement of thermonuclear fusion with the gain coefficient $E_{THF}/E_L \sim 1\text{-}10^3$ it is necessary to attain a laser beam energy $E_L \gtrsim 10^4\text{-}10^6$ J with a pulse length of $\tau_L \gtrsim 10^{-1}\text{-}10$ ns. In addition, the laser beams in these systems should possess the following specific properties: a high level of radiation contrast ($\sim 10^7\text{-}10^9$), low beam divergence ($\sim 10^{-3}$), multiple-beam output, synchronization of optical paths, and possibility to vary the pulse shape and length.

As was shown in Ref. 27, in actual multichannel laser systems the output energy E_L is bounded on one side by conditions dictated by the increase of beam divergence with the increasing number of amplification stages, and on the other side by the necessity to heat a prescribed target mass to the required specific internal energy level. In addition to these requirements, the obtainable laser energy output depends essentially on the construction scheme of high-energy amplification stages, which, to a large degree, determines the attainable beam divergence, on the energy deposition regime and on the detailed structure of the target. The necessity of high radiation contrast level follows from the necessity to effectively heat thin-walled targets which can be vaporized with a prepulse energy of as little as $\sim 10^{-3}$ J. The requirements of a multichannel system and optical path synchronization follow from the necessity to achieve a high degree of spherical symmetry in target irradiation ($\sim 1\%$), which is necessary[20,24,25] to attain high compression.

Above considerations were taken into account in the construction of the here-described high-energy, 12-channel laser system, DELFIN, built of Nd:glass and intended for spherical heating of thermonuclear targets. The purpose of this laser system and associated diagnostic apparatus is a broad investigation of the physics of laser-plasma interaction, optimization of target heating, and experimental demonstration of thermonuclear yield that is high, relative to the beam energy (0.01-1.0) deposited in the target. At the present time the first leg of the system is being assembled. It is intended to generate three beams with the energy of ~ 3 kJ.

Among different schemes for the construction of powerful laser systems[3,27] the most effective is the one with series-parallel composition of high-energy amplification stages in which equality is maintained between the beam splitting coefficient and the amplification coefficient of individual stages for high-energy input signals. The DELFIN system described here is constructed according to such a scheme in which $K \gtrsim 3$, $n = 2;3$. The fundamental block diagram of the DELFIN scheme is shown in Fig. 1, and the general view of the optical room containing the laser system (excluding the capacitor bank) and the vacuum chamber with diagnostic instrumentation is shown in Fig. 2. Two types of pulse generators (ZG) with a system of electro-optical gates allow formation of light pulses with a length of $\sim 10^{-10}\text{-}10^{-9}$ s and energy of 10^{-5} J. The laser system allows, when

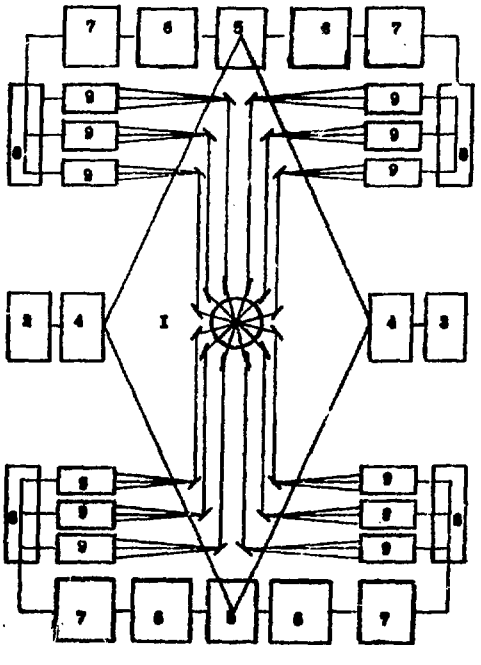

Fig. 1. Principal block diagram of the high-energy laser facility DELFIN. (1) vacuum chamber; (2) nanosecond pulse generator; (3) subnanosecond pulse generator; (4) LPKA; (5) PKU; (6) PKUII and PKUI; (7) MKUII and MKUIII; (8) splitting and compensating system; (9) VKU.

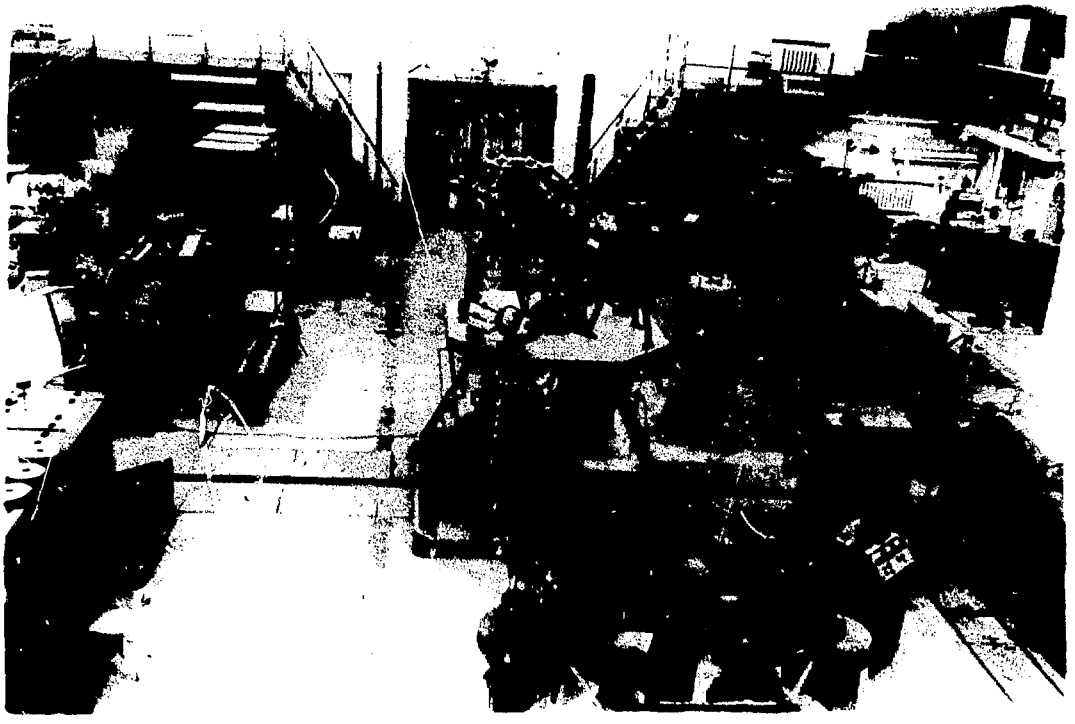

Fig. 2. General view of the optical hall.

necessary, an increase in the pulse length to 10^{-8} s. These pulses are amplified to the energy of ∿ 50 J in a linear system of preamplifiers (LPKU) with an exit aperture of 45 mm. Further amplification is achieved in preamplifiers (PKU I-II) and also in high-energy and final amplification stages (MKU I-III and VKU I-III) with a series-parallel addition of active elements; here the flux density is near the ultimate ($q \gtrsim 3$ GW/cm^2 for τ_L = 1 ns), $K \gtrsim 3$ and $n \leq 3$. In each of the twelve VKU there are 18 active elements with axes so oriented as to ensure convergence of each beam to an aperture of 270 mm located on a single plane at a prescribed distance from exit windows. In this plane are placed multiprismatic mirrors which, from 18 parallel beams of 45-mm diameter each, form composite beams (SP) with apertures not exceeding 270 mm. Total laser radiation energy in SP reaches the value ∿ 0.4-0.8 kJ depending on the length of the amplified light pulse. Twelve SPs are formed at the exit with the total laser radiation energy ∿ 10 kJ. The expected radiation beam divergence is $\alpha \gtrsim 5 \times 10^{-4}$ rad and brightness $B \gtrsim 3 \times 10^{15}$ W/cm^2, which corresponds to a maximum flux density at the target of $q \gtrsim 10^{15}$ W/cm^2.

PULSE GENERATOR

Light pulses of subnanosecond length are formed in a Nd:YAG laser system employing a periodic cavity Q modulation.[29] The basic scheme of the oscillator is shown in Fig. 3. Optical length of the resonator L_p is 237 cm. Selection of the fundamental transverse mode is accomplished by means of a diaphragm with a diameter of 2 mm. A Pockels cell with crystal DKDP (10 x 10 x 25 mm^3) and a Glan-Thompson prism is used to modulate loss in the resonator. The cell is controlled externally with a ruby laser and a laser-triggered spark gap. Periodically occurring ($T = 2L_p/c$), where c is the speed of light) deep modulation of the cavity Q-factor results in the generation of a pulse train with length ∿ 0.3-0.4 ns but with a ∿ 16-ns separation between individual pulses. Selection of an individual pulse from the train is accomplished by switching the Pockels cell with a laser-initiated discharge (RLP). To improve the

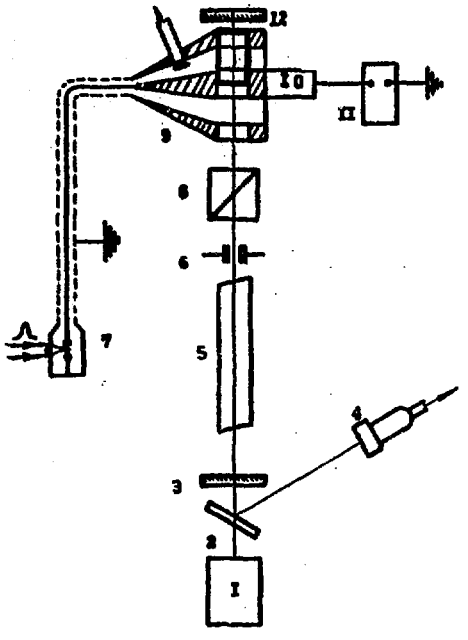

Fig. 3. Pulse generator scheme with periodic modulation. (1) streak camera; (2) optical plane; (3) mirror (14); (4) photocell; (5) active element; (6) diaphragm; (7) laser-triggered spark gap; (8) Glan prism; (9) Pockels cell with DKDP crystal; (10) charge resistor; (11) high-voltage power supply.

temporal characteristics of the pulse selection scheme the laser radiation is preamplified in a one-stage two-pass amplifier which allows an increase in the accuracy of synchronization between gate operation and laser pulse arrival and significantly reduces the transmission window of the gate. The last is most important for the attainment of high values of the radiation contrast. As a consequence there is formed at the exit from the system a single laser pulse with the above-indicated length, with energy $E_L \approx 10^{-1}$ J, and with a diffraction-limited beam divergence $\alpha = \alpha_d$ with a beam diameter D = 2 mm.

Formation of light pulses of nanosecond length is accomplished by means of a single-mode Nd:glass ZG oscillator employing active Q-switching. The layout of ZG and the preamplifier stages LPKU are shown in Fig. 4. The Q-switch is turned on by closing a discharge-operated Kerr cell located inside the resonator and operated with the RLP generator of Rb crystal used for diagnosing the laser plasma (light source for optical diagnostic methods). The resonator has a base length L_p = 120 cm. Discrimination of the transverse modes in the resonator is accomplished with a diaphragm of 2-mm diameter located near the output mirror. The total passive radiation losses inside the resonator in the open

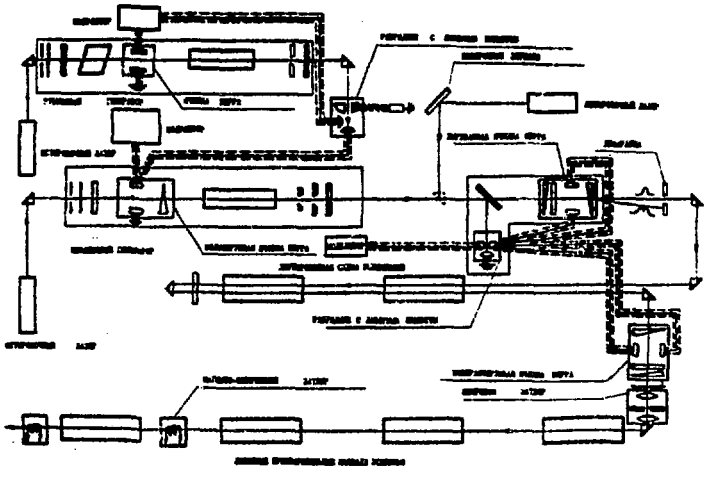

Fig. 4. Scheme of the nanosecond pulse generator and of the linear preamplification stages (LPKU).

state do not exceed 10%. Such a generator allows us to obtain an output radiation pulse of length τ_L = 30 ns with energy E_L = 0.5 J. Divergence of the radiation is diffraction limited and corresponds to that limit for a light pulse of 2-mm diameter.

The necessary nanosecond length of the laser pulse is ensured by the pulse forming system including fast electro-optical closing of the Kerr cell and the RLP. A special high-voltage Kerr cell (∿ 70 kV) with a double controlling signal is used to increase the speed of the system. The construction of the cell allows a several-fold increase in the speed of rotation of the plane of polarization of the laser light and ensures a stable pulse formation of length $\tau_L \approx 0.5$ ns.

It is necessary to devote special attention to the achievement of the required value of radiation energy contrast K_E, which is basically determined by the construction of the thermonuclear target (dimension, material density, sublimation energy, absorption coefficient for laser radiation) and the energy level of light radiation. For laser radiation energy $E_L \sim 10^4$ J for heating of microballoon targets, the required quantity K_E can reach values of 10^7-10^8. The energy contrast is described by the expression

$$K_E = \frac{E_L}{E_{ph1} + E_{ph2}}, \qquad (1)$$

where E_L is the energy of the short laser pulse heating the plasma, E_{ph1} is the photon energy during pumping, E_{ph2} is the radiation photon of the pulse generator. The quantity E_{ph2} can be reduced relatively easily to a prescribed value with the application of different decoupling devices[30-32] (electro-optical gates, Faraday gates, clearing filter, clearing films, etc.), located between separate stages. Concerning a photon in ZG-E_{ph2}: reduction of this quantity and consequent achievement of the required contrast with respect to the radiation from the generator is a complex problem related to the development of high-contrast, fast-acting electro-optical gates with subnanosecond response time.

In the facility being described, application of the Kerr cell with a duplex control signal in combination with wedge-shaped polarizers of Icelandic spar immersed in nitrobenzene, which decreases depolarized radiation, makes it possible to achieve a contrast of $K_E \approx 10^5$. For further contrast enhancement, there is placed in the LPKU system a second analogous Kerr cell gate with a larger aperture (D ∿ 1.5 cm), which is synchronized with the first one. The gates are operated with a single RLP placed in a high-pressure nitrogen atmosphere (P = 10-15 atm). The shortest response time for the gates is ∿ 0.2 ns, synchronization accuracy is ∿ 0.05 ns, jitter in synchronization with the laser pulse does not exceed 1 ns. The above-described system allows achievement of contrast $K_E \sim 10^8$.

LINEAR PREAMPLIFIERS (LPKU)

Pulses formed in the "slicing" system are amplified in a six-stage amplifier (see Fig. 4) whose first two stages operate in the two-pass amplification regime. Nd:glass rods, 45-mm diameter and 560-mm active length, are used in all stages of LPKU of the DELFIN facility. To supress generation and amplification of parasitic oscillations, faces of active elements are cut at an angle of 85° with respect to the axis. The standardization of active elements in LPKU does not reduce the total gain in the system because energy present in LPKU amounts to not more than 2% of the total energy of the system.

Saturable absorbers and magneto-optical Faraday gates are utilized to optically decouple amplifiers. In addition, after the two-pass amplifiers there is located an optical spark gap[33] consisting of a combination of a slow (low light-gathering power) positive lens and a diaphragm of diameter ∿ 0.5 mm located at its focus. For light pulses with length not exceeding several nanoseconds, such a system is a very effective decoupler with small optical losses. It is appropriate to note that, in addition to optical decoupling, such an arrangement ensures protection of the ZG and the pulse formation system from the damage by the laser pulse reflected off the target and amplified in all preceeding stages.

In order to minimize the effects of self-focusing in the active elements that damage the optical medium and reduce beam quality, high-intensity laser radiation is amplified in a divergent beam. All optical elements of the LPKU system are carefully controlled with respect to the homogeneity of the optical glass and finish of the optical surfaces. The importance

of this control follows from considerations presented in Ref. 27. Control is achieved by means of a schlieren method with automatic registration of the optical quality. The quality criterion is the ability of the optical elements to operate on beams in the diffraction-limited regime. The pumping in LPKU is carried out at energy levels considerably lower than in MKU and VKU systems in order to minimize distortion of active elements during pumping. Compensation for thermal lens effects occurring in the rods is accomplished with special corrective optical elements located at the exit from the LPKU. The parameters of the corrective optics are determined from measurements of the structure of the wave front of laser radiation. These measurements, with the accuracy down to λ, were carried out with the aid of holographic methods based on the interference of an ideal plane wave of diffraction-limited divergence with the resulting actual laser beam.

The above-enumerated precautions enabled us to obtain at the exit from LPKU a laser beam with the following parameters: radiation energy $E_L \approx 30$ to 50 J with light radiation pulse width $\tau_l \approx 1$ ns; the total angle of beam divergence in which 90% of the energy is concentrated, $2\alpha \approx 2 \times 10^{-4}$ rad; radiation brightness $B \approx 6.5 \times 10^{16}$ W/cm^2 ster; energy contrast $K_E \approx 10^8$.

PKU, MKU, AND VKU SYSTEMS

The laser beam, after leaving LPKU and being reconditioned, enters series-parallel amplifiers, where it gains most of its energy. The following specific problems must be solved to construct MKU with a system of series-parallel amplifiers: selection of the optimum coefficient for beam splitting, compensation for optical path lengths of different beams, self-excitation in stages of circular resonators, etc. The construction principle of the MKU scheme depends largely on solutions of these problems. In the here-considered DELFIN facility an industrial-type illuminator GOS-1001 with an active element of Nd-glass GLS-1 with 45-mm diameter and 560-mm active length is used as a standard amplification element. Four flashlamps IPhP-20000 are used for pumping; maximum pumping energy for the illuminator is ~ 50 kJ with the discharge current pulse length of ~ 5×10^{-4} s. Under these conditions the amplification coefficient for laser radiation with energy flux density $q \geq 1$ GW/cm^2 at the exit face of the rod does not exceed $K \approx 3.5$. This quantity imposes a bound on the beam-splitting coefficient in strong amplifiers. To obtain maximum coefficient of laser efficiency with respect to the stored electrical energy, it is necessary to perform amplification under saturated gain conditions.[3] In other words, the amplification region in which the beam at the entrance to the stage is first immediately divided into the necessary number of channels and then all channels amplified simultaneously in many parallel amplifiers is energetically less convenient because, in this case, the energy extraction from active elements at the beginning of the stage is extremely small (of the order of a few percent) while the pumping energy in the general balance may reach 80 to 90%. In such schemes there appear, in addition, complications in the solution of problems connected with the attainment of high contrast in emission.

In the facility being described here, there was adopted a scheme for staged beam splitting (see Fig. 5) with the following multiplication coefficients for individual stages: n = 2; 2; 3; 2; 3; 3. With such multiplication scheme the number of beams grows as 1 → 2 → 4 → 12 → 24 → 72 → 216. The use of n = 2 in the middle link MKU is connected with the necessity to compensate for the energy losses incurred in transporting the beam to the entrance of MKU and in the elements of the system which split the beams. The general view of MKU I-III and of VKU is shown in Fig. 6. Also seen in that figure are collimators of the cylindrical optics used for beam splitting, which allow the change of the geometric cross section of the beam, and divide it into two energetically equal parts. The change in the coefficient of beam splitting is accomplished by varying the magnitude of the linear beam transformation. In this scheme the energy losses of the laser pulse amount to 8% and nonuniformities in beam division including, also, effects of actual divergence and optical path lengths between amplification stages do not exceed a few percent. Final amplification of laser radiation occurs in the active elements VKU, three of which are shown in Figs. 7 and 8. Each stage is a module of 18 illuminators with the overall dimensions 85 x 100 x 170 cm^3 (Fig. 9). The DELFIN facility contains 12 such

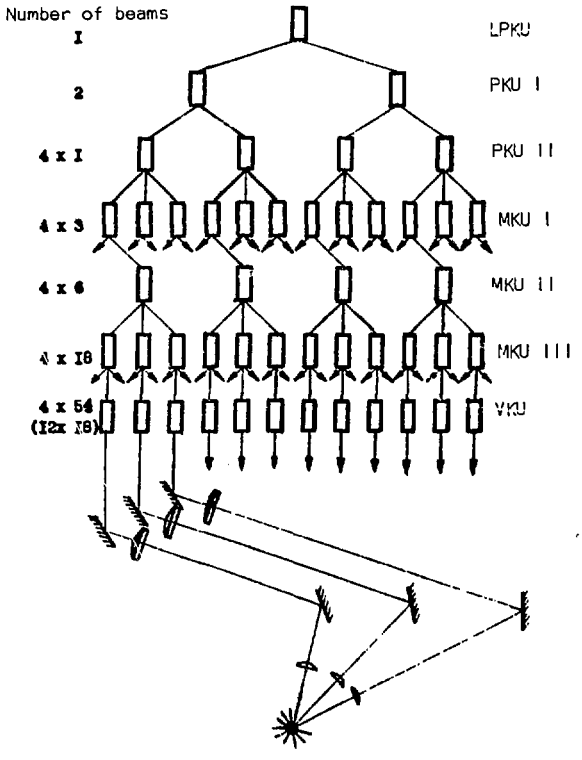

Fig. 5. Beam splitting scheme.

VKU modules and its output consists of 216 laser beams of equal energy density, each 45-mm in diameter. In principle these beams can be combined downstream by various methods depending on the illumination scheme of the thermonuclear target.

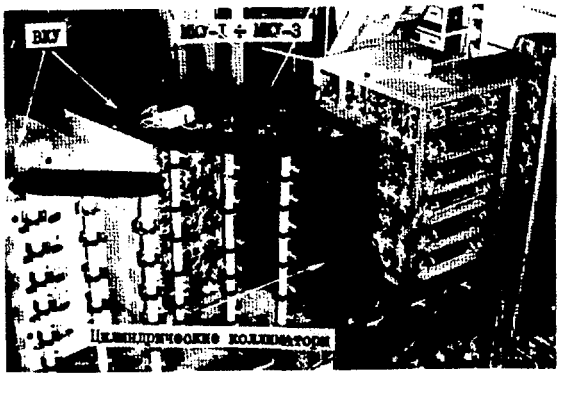

Fig. 6. General view of MKU I, II, III, VKU, and cylindrical collimators.

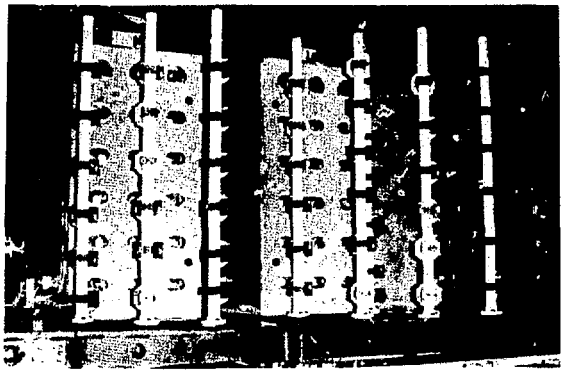

Fig. 7. General view of VKU from the MKU side.

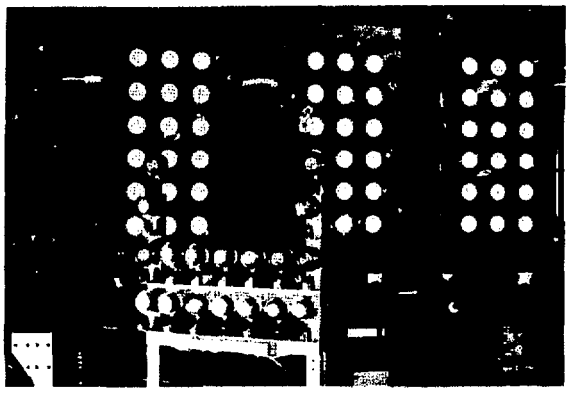

Fig. 8. General view of VKU from vacuum chamber side

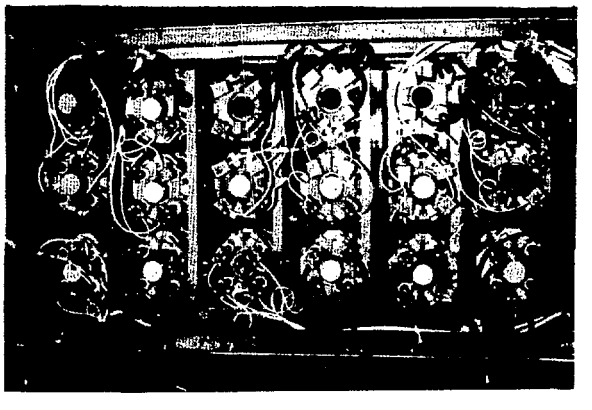

Fig. 9. Arrangement of laser amplifiers in VKU module.

TABLE I

DELFIN AMPLIFICATION STAGE PARAMETERS

Stage Designation	Number of Beams	Cross-Section Area	Amplification Coefficient	Energy (J)	Energy Density J/cm^2	Beam Divergence (rad)	Brightness W/cm^2 ster
LPKU	1	15	1.5×10^4	30	2.0	1×10^{-4}	6.5×10^{16}
PKU I	2	30	2.3	70	2.3	---	---
PKU III	4	60	2.6	180	3.0	---	---
MKU I	3	45	3.3	120	2.7	---	---
MKU II	6	90	3.4	320	3.5	2×10^{-4}	2.8×10^{16}
MKU III	18	270	3.4	880	3.25	---	---
VKU	3 x 18	810	3.6	2500	3.1	5×10^{-4}	4×10^{15}
Facility Output Parameters	12	3240	---	10^4	---	5×10^{-4}	3×10^{15}

The basic parameters for different amplification stages of the DELFIN high-energy laser facility are presented in Table I.

THE SCHEME FOR FOCUSING RADIATION ON THE SPHERICAL TARGET SURFACE

It is not possible to make any definite conclusions about the focusing requirements for multichannel lasers with output energy levels of $E_l \approx 10^4$ J and higher on the basis of the presently available publications about the experimental realization of spherical irradiation of solid targets (see Refs. 3, 6, 10, and 34) because of large differences in experimental conditions and relatively low laser-energy levels. Therefore, it is interesting to analyze the specific action of the focusing optics and to examine the requirements on the parameters and construction details of the focusing elements that follow from it.

As was noted in Ref. 27, in laser fusion experiments the energy level of light emission is directly related to the effective size of heated targets. At thermonuclear temperatures when the specific internal plasma energy is $E \approx 10^8$ to 10^{10} J/g, the maximum allowable dimension of solid targets amounts to only a few tens of micrometers. Use of hollow (membrane) targets allows a considerable increase in the target size. Characteristic dimensions of targets of different constructions corresponding to different laser energies are given in Ref. 27.

For effective target heating it is necessary that the minimum diameter of the caustic, d_{min}, defined by the relation

$$\int_0^{d_{min}} E(r)dr = \psi \int_0^{\infty} E(\tau)d\tau \qquad (2)$$

does not exceed the target diameter, i.e., $d_{min} \leq 2r$. In Eq. (2) E(r) is the far field laser beam energy distribution, and ψ is the overlap coefficient which determines the allowable energy loss in focusing, whose value is determined by the conditions of the experiment and can reach $\psi \approx 0.95$. A decrease in ψ leads to a decrease in energy density of the radiation beam and consequently to a bound on the attainable values of plasma parameters.

Under these conditions, when heating massive spherical targets with laser beams with energies of 10^3 to 10^4 J, it is necessary that the diffraction-limited abberation spot size of the focusing optics does not exceed 50 to 60 μm. Use of thin, hollow target models which allow larger target sizes, however, is accompanied by increasing restrictions on the values of temporal and spatial departures of the surface irradiation from certain mean values (in the units of beam energy density this mean value is $q \approx 10^{14}$ W/cm^2), which for targets with thickness

to radius ratio of $\sim 10^{-2}$ should not exceed a few percent. Realization of the almost uniform spherical irradiation of an isolated target with a limited number of light beams requires construction of a focusing scheme which allows variation within wide limits of the far-field laser beam intensity distribution while strictly satisfying condition (2). With respect to the focusing optics this means that the diameter of the diffraction-limited abberation spot should be considerably less than the target diameter ($r_{abb} \approx 0.1\ r$) and for a laser facility with the energy level of $\sim 10^4$ J it should not exceed 60 μm, i.e., $r_{abb} \lesssim 60\ \mu m$.

It is necessary to note that high-energy laser beams present specific conditions for the operation of optical elements which limit the possibilities for application of known focusing methods. Most important in this connection is the necessity to take into account the beam stability in glass, E_{pr}, which imposes a condition on the minimum aperture size of the elements used for focusing which, in turn, in the case of spherical irradiation geometry leads to a lower bound on the magnitude of the focal length S. Indeed, the aperture of the individual element D of the focusing scheme for a multibeam laser containing N beams that fill the target surface with fill coefficient μ is connected to the radiation output energy with the following relation:

$$D = 2\left(\frac{E_L}{\mu\pi N E_{pr}}\right)^{1/2}. \qquad (3)$$

Obviously, the total solid angle of the laser radiation convergence on the target should not exceed a certain limiting value Ω which, with the condition $D \ll S$ that is satisfied for high-energy laser systems, can be expressed in the form

$$\frac{\pi N D}{4S^2} \leq \Omega. \qquad (4)$$

Substituting expression (3) into inequality (4) we obtain a bound on the focal length

$$S \geq \left(\frac{E_L}{\mu E \Omega}\right)^{1/2}. \qquad (5)$$

(Translator's note: algebra does not check!)

It is also easy to obtain a bound on the magnitude of the light gathering power (speed)(D/f) of the individual objective

$$\frac{D}{f} \leq \frac{D}{S} \approx 2\left(\frac{\Omega}{\pi N}\right)^{1/2}. \qquad (6)$$

In this way the basic characteristics of the focusing objectives are uniquely determined by the parameters Ω, N, and E_L. Some remarks about these quantities are in order.

In facilities with energies between the limits $E_L = 10^3$ to 10^4 J the solid angle of the radiation convergence onto the target is bounded mainly by the construction details of the vacuum chamber and of the focusing systems. These are: the large number of diagnostic windows in the walls of the vacuum chamber, apparatus for target placement and for the focusing of laser beams on its surface, components of the vacuum system, etc. An essential restriction on the quantity Ω is imposed by the conditions of minimal optical coupling of separate amplification channels through the target, i.e., penetration of radiation diffracted by the target into another focusing channel. To satisfy this condition it is necessary to arrange the optical axes of the objectives in such a way that the light cones of the incoming and outgoing beams at the target do not overlap. All of the above considerations lead to the conclusion that Ω should not exceed 1/5 to 1/6 of the full solid angle; for actual conditions it is advisable to require $\Omega \lesssim 0.1$ to 0.05.

Another important parameter of the MLU is the number of channels for the irradiation of the target. As can be seen from Eqs. (3) and (6), an increase in the number of channels allows a significant reduction in the requirements on the parameters of the objectives. However, an increase in the number of focusing channels leads to a rapid increase in the total number of adjustable coordinates and optical elements, which inevitably lowers the reliability of the entire system. It appears that it is not suitable to increase the number of channels above several tens. The number of channels is bounded from below by the necessity to achieve a high degree of uniformity in the irradiation. Apparently the smallest value of N for which a uniform irradiation can be obtained (within a few percent error) is $N \geq 4$. Therefore, the optimal value of N should be chosen in the interval $4 \leq N \leq 30$.

Above presented considerations are illustrated graphically in Fig. 10 where, for laser systems with different numbers of channels and different Ω and μ, plotted is the dependence of the required aperture of the focusing objective (continuous curves labeled "A"), and of the magnitude of the focal length (dotted lines labeled "B") on the laser energy, and also the dependence of the relative aperture on the angle of convergence of radiation onto the target ("C").

These estimates show that the requirements on the most difficult to achieve objective parameter, light-gathering power, decrease substantially with increasing laser-focused energy. This circumstance allows consideration of different types of focusing objectives for facilities with different output energies. In facilities with moderate values of laser radiation energy, $E_L = 10^3$ to 10^4 J, the use of single-component espherical objectives appears most appropriate. For the focusing of radiation with energies $E_L = 10^5$ to 10^6 J, the application of simple spherical one- and two-lens systems may become possible.

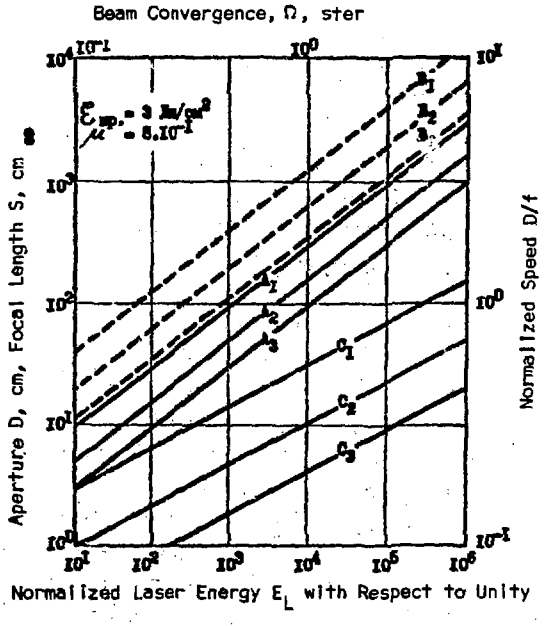

Fig. 10. Dependence of the focusing lens aperture D (solid curves marked "A") and the focal length S (marked "B") on laser energy. The dependence of D/f on the convergence of laser radiation on the target (marked "C"). "A_1"-N=4; "A_2"-N=12; "A_3"-N=30. "B_1"-Ω=π/25; "B_2"-Ω=π/6; "B_3"-Ω=π/2. "C_1"-N=4; "C_2"-N=12; "C_3"-N=30.

In addition to what has been said above, there are a number of supplementary requirements on the characteristics of separate elements of the focusing system. This is, first of all, protection of the optical elements of the focusing system from damage by the focused radiation reflected off the optical surfaces. At the present time this problem is solved by the methods based on the exclusion of the central core of the beam (opaque cover on central portions of the lenses, drilling central holes, formation of ring-shaped laser beams, etc.)[35] which, when combined with high-transmission coatings, is sufficient for the entire focusing system.

Another important problem is ensurance of least optical coupling between the amplification stages of the laser system and the focusing objectives. This condition is connected with the necessity to attain high values of radiation contrast at the facility output and is the principal necessity in laser initiated thermonuclear systems. Small signal gain in lasers with energies $E_L \approx 10^3$ to 10^4 J reaches values ~ 10^{10} to 10^{11}; therefore, even the use of several sequential electro-optical gates does not guarantee nonoccurence of parasitic oscillations. It appears that the coupling coefficient should not exceed the value ~ 10^{-3} to 10^{-4}, and to attain such values transmission through optical surfaces alone appears insufficient. It is also necessary to select a definite surface shape for the lenses and to combine the optical elements in such a way that all beams reflected toward the laser aperture are strongly divergent.

All of the above considerations were taken into account in the construction of the focusing system used in the here-described MLU.

The focusing system consists of 12 channels, each of which contains a multiprism mirror, a two-component objective, a prism system of large aperture for beam turning, and a complex of devices for assembly and adjustment. The general arrangement of optical elements in the focusing system is shown in Fig. 11.

The coordinate locations of separate elements and intersection points are given in Table II. Eighteen beams of 45-mm diameter from the exit of each of the 12 VKU modules are directed onto a multiprism mirror (see Fig. 12), which combines them into

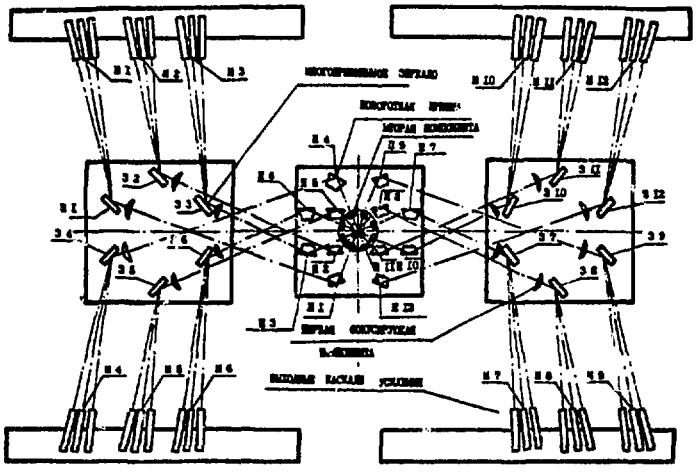

Fig. 11. Layout of the optical elements in the focusing system.

TABLE II

No.	Element Designation	Coordinates of Center x	y	z
1	M 1	-7738	+4130	0
2	M 2	-6775	+4125	0
3	M 3	-5860	+4118	0
4	M 4	-7738	+4130	0
5	M 5	-6775	-4125	0
6	M 6	-5860	-4118	0
7	M 7	+5860	-4118	0
8	M 8	+6775	-4125	0
9	M 9	+7738	-4130	0
10	M 10	+4860	+4118	0
11	M 11	+6775	+4125	0
12	M 12	+7738	+4130	0
13	3 1	-6800	+ 370	0
14	3 2	-6100	+ 855	0
15	3 3	-5500	+ 400	0
16	3 4	-6800	- 370	0
17	3 5	-6100	- 855	0
18	3 6	-5500	- 400	0
19	3 7	+5500	- 400	0
20	3 8	+6100	- 855	0
21	3 9	+6800	- 370	0
22	3 10	+5500	+ 400	0
23	3 11	+6100	+ 855	0
24	3 12	+6800	+ 370	0
25	11 1	- 456	- 846	-276
26	11 2	- 276	- 276	+921
27	11 3	- 846	- 456	-276
28	11 4	- 456	+ 846	+276
29	11 5	- 276	+ 276	-921
30	11 6	- 846	+ 456	+276
31	11 7	+ 846	+ 456	-276
32	11 8	+ 276	+ 276	+921
33	11 9	+ 456	+ 846	-276
34	1110	+ 846	- 456	+276
35	1111	+ 276	- 276	-921
36	1112	+ 456	- 846	+276

a single beam of aperture D_1 = 285 mm, energy E_1 $\approx$ 1 kJ, divergence $2\alpha \approx 10^{-3}$ rad, and pulse length $\sim 10^{-9}$ s with a time-scatter of light pulses because of the differences in optical path lengths of individual 45-mm diameter beams within the limits $\Delta\tau \leq 30$ ps.

Shown in Fig. 13 is the structure of the resulting beam and Fig. 14 is the target irradiation geometry. In Table III are listed the values of angles defining spatial locations of the axes of the focused beams. The coordinate system in Fig. 14 is rotated by 45° in the counterclockwise direction about the z-axis with respect to the coordinate system of Fig. 11.

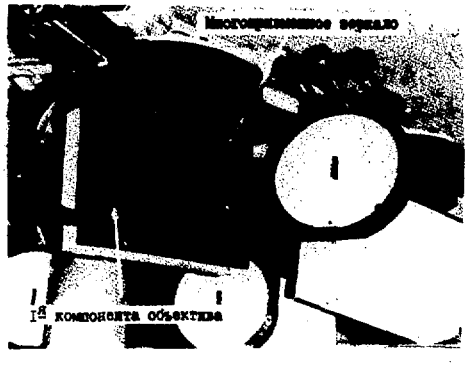

Fig. 12. Multiprism mirror and the first focusing lens.

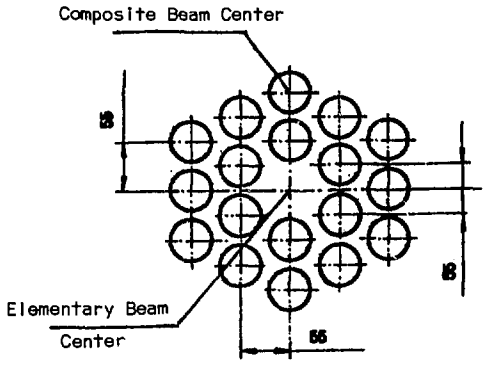

Fig. 13. Composite beam structure.

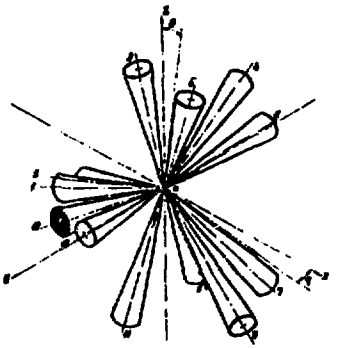

Fig. 14. Geometry of target illumination.

At the present time the component beams are focused with two-lens objectives (Fig. 15). The first lens with the focal length of $f_1 = 10^3$ cm is mounted on a special stand near the multiprism mirrors (see Fig. 12). The second lens with focal length $F_2 = 230$ mm is mounted in the wall of the vacuum chamber and simultaneously serves as a vacuum window. The aberration diameter of the caustic of the focusing system is $d_{ab} \approx 300$ μm. There are provisions in the focusing system for the axial displacement of the long focal length element, to obtain a longitudinal variation of the plane of the minimum caustic and the necessary orientation of beam axes, and their spatial distribution relative to the target surface is achieved with a totally reflecting prism located in an adjustable frame at the distance of 1 meter from the target. The limiting radiation flux density at the target surface attainable with the laser system containing the above-described focusing system reaches the value $q \approx 10^{15}$ W/cm^2.

The characteristic property of the modular focusing system is the use of one optical element to focus many laser beams (a module). The modular system has many advantages over the multilens system, in which for each beam a separate focusing and turning element is provided. Thus, for the DELFIN facility being considered, instead of 216 focusing elements (objectives) only 12 are used, which significantly facilitates focusing and increases system reliability. In addition, use of multiprism mirrors allows scanning with the elementary laser

TABLE III

Number	θ	ψ
1	106°	64°
2	23°	180°
3	106°	196°
4	74°	254°
5	151°	270°
6	74°	286°
7	106°	344°
8	23°	0°
9	106°	16°
10	74°	74°
11	157°	90°
12	74°	106°

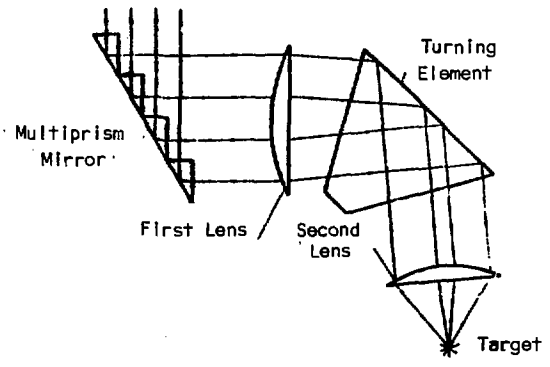

Fig. 15. Two-lens modular focusing system.

beam in the plane of the target in order to achieve a definite intensity distribution on its surface. The main disadvantages of the modular system are the necessity to use beam-turning elements with large overall dimensions and a longer optical path inside the glass, which may have a detrimental effect on the radiation parameters. Also, when a single-component modular system is used, there appear complications in scanning with the focusing lens in three-dimension.

The two-lens modular scheme used in the DELFIN facility allows a reduction of the overall dimensions of the turning element relative to the single-lens system and a simplification of the procedure of focusing radiation onto the target surface. Adjustment of the position of the focus in the target zone is accomplished with an immovable short-focus component by scanning over two angular coordinates with the turning element and along the beam direction with the long-focus lens.

The chief disadvantage of the system is high-energy flux density at the output element $q \approx 4$ GW/cm^2.

In concluding this description of the focusing system, we note that it would be advantageous to increase the number of beams in each separate light module and to focus them on the target with a large-aperture-angle element, because this would facilitate attainment of high uniformity in irradiation. In this connection of interest is the mirror focusing scheme shown in Fig. 16. Four elliptic mirrors are placed around the target with tetrahedral symmetry, laser radiation is focused into one of their focuses with a low light-gathering power lens (1:10). Second focuses of the elliptic mirrors are colocated with the center of the target (Fig. 17).

Radiation is concentrated in the forward (first) focuses with multiprism mirrors colocated with a multilens spherical segment. Such focusing system allows attainment of spherically symmetric target irradiation with the total aperture angle $\Omega = 3\pi$. A property of this scheme is the absence of aberration, which allows formation of the focal spot with dimensions determined by laser beam divergence. The system can be adjusted with the aid of multiprism mirrors while keeping elliptic mirrors fixed.

Difficulties in constructing such a scheme are connected, basically, with difficulties in producing aspherical mirrors with large diameters (D_{mirr}

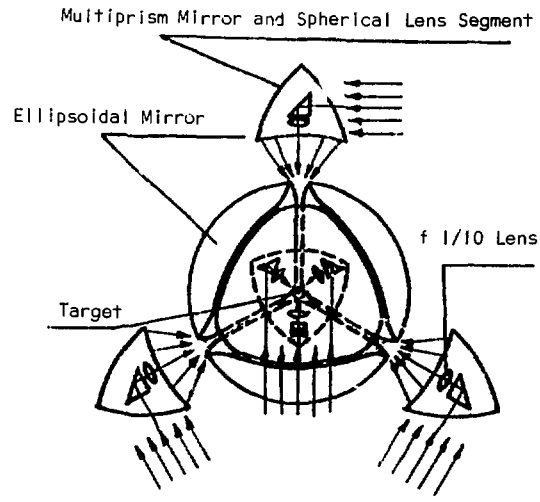

Fig. 16. Focusing system using multiprism mirrors.

$\approx$ 600 mm), and in obtaining uniformly homogeneous surface coatings.

It is appropriate to note that an analogous system for two simple beams was employed in the work described in Ref. 24.

THE CONTROL SYSTEM

The DELFIN facility contains a large amount of control and diagnostic apparatus and supporting instrumentation (including commercially manufactured items) used to run the facility and to control its

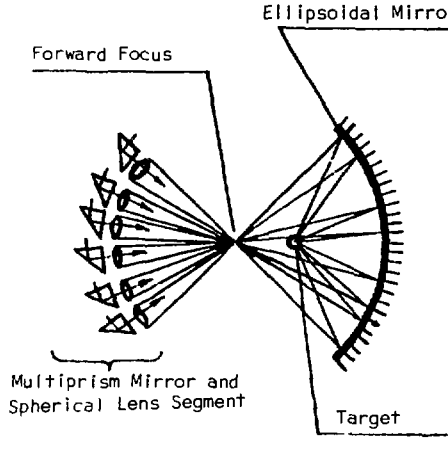

Fig. 17. Operating principle of ellipsoidal mirrors.

basic parameters. This collection can be divided into several functional groups:

1. Instrumentation of the energy supply system for the neodymium glass laser (control and ...ication of charge in the capacitor bank, power transformers, discharge and synchronization of the bank discharge through flashlamps, etc.);
2. Apparatus and mechanisms used for laser adjustment and for the focusing of radiation on target (gas lasers with emission wavelength λ = 1.15 μm, 0.63 μm, YAG-lasers, electro-optical transformers, optical systems, etc.);
3. Measurement and control instrumentation for radiation emission from the strong laser, including the complex of multichannel calorimeters, fast oscillographs, laser radiation detectors with feed cables, streak cameras, etc.; and
4. Diagnostic apparatus for the thermonuclear plasma.

Assurance of reliable performance of the entire system, and its control in accordance with a prescribed plan is a problem in itself. Its solution requires a single automatic control system based on the application of electronic computers. Taking into account the multiplicity of functional schemes for the automatic control of systems that ensure satisfactory operation of the laser facility (control of electronic and electric devices, pneumatic and thermal devices, electromechanics and optics, etc.), and the large information flow transmitted from them to the operator during a short time interval (~ 10 min), it is planned to construct the automatic control system based on the CAMAC standard with the application of the fast electronic computer of the type NOVA 2/10 with large operating and storage memories.

This approach allows considerable reduction in time necessary to construct the automated control complex because the wide application of standard CAMAC modules reduces the quantity of required new developments. A second advantage is the fact that in this way there exists a possibility for a stepwise solution of all problems and for a continuous increase in power of the automatic control system by the addition of new systems. The automation of the target placement system in the vacuum chamber, and of the adjustment system for the focusing optics are planned as the first stage of the work toward construction of automatic control system for the DELFIN facility.

VACUUM CHAMBER AND DIAGNOSTIC INSTRUMENTATION

The vacuum chamber is a stainless steel hollow sphere with inside diameter of 460 mm and outside diameter of 520 mm outfitted with different diameter windows (Fig. 18). The vacuum chamber is intended for target mounting either in vacuum or in a gas at a prescribed pressure, for the location of apparatus for target alignment, for the mounting of the focusing optics, and of the diagnostic instrumentation. The vacuum attainable in the vacuum chamber is $p \approx 10^{-6}$ mm Hg.

The target mounting system ensures location of hollow and solid spherical targets at the center of the vacuum chamber with the accuracy $\Delta_{xyz} = \pm 5$ μm in all three coordinates. A scheme is provided for the location of up to five targets in the chamber without breaking vacuum. Each target is independently attached to the adjusting mechanism with a polymer thread of 1- to 5-μm thickness.

Observation of the target position in the chamber is with the aid of two crossed long-focus microscopes with magnification X40, which allow control of the position of the target with prescribed accuracy. The control can be accomplished either directly at the vacuum chamber or remotely from the experiment control panel with the aid of a television camera.

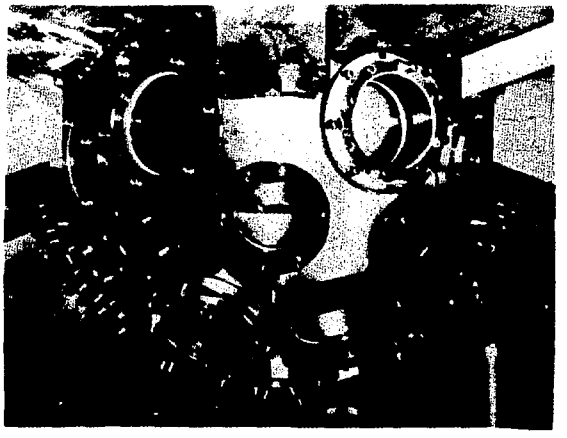

Fig. 18. View of the vacuum chamber (top hemisphere).

In addition, the mechanism for target adjustment is provided with a system that allows target adjustment either remotely with telemeter control or automatically with the aid of a special target tracking and position computation system. The apparatus for automatic adjustment consists of a sectional photoelement, target illumination system, an optical system that magnifies and transmits the target image onto the cathode of the photoelement, a signal impulse forming scheme, and a feedback connection system. An electrical signal proportional to the magnitude of target displacement relative to the prescribed position is imposed on servomechanisms which calculate target coordinates with the accuracy of ± 5 μm.

Search and location of the target is carried out in a spherical volume of ~ 0.125 cm^3. The maximum time required for position determination is ~ 3 min. In practice the same length of time is needed to place the target into position from those already located inside the vacuum chamber.

Fundamental diagnostic problems for thermonuclear laser plasma are the investigation of the absorption processes for laser radiation in the corona region ($M_e \leq 10^{21}$ cm^{-3}),[13,14,36,37] and the transformation processes of the absorbed radiation into thermal energy of ions, both in the corona region and in the compressed plasma core of the target ($M_e > 10^{22}$ cm^{-3}),[3,10,38] where the thermonuclear burn is initiated at a sufficiently high density and temperature.

In high-temperature heating of the plasma with laser radiation the energy absorbed in the target is transformed mainly into kinetic energy of both directed and random (thermal) motions of the plasma particles and into energy of x-ray emission from the plasma. From the point of view of laser-induced thermonuclear fusion, useful processes are transformation of the energy of electrons which absorb laser radiation (bremsstrahlung absorption) into kinetic energy of the ordered motion of ions toward the center of symmetry, which leads to target compression and into the energy of thermal ion motion in the dense plasma. Parasitic processes which lower the effectiveness of target heating and compression are energetic x-ray emission from the plasma[3,10,39,40] and formation of streams of highly energetic (super-thermal) electrons[13,43-47] or ions[48-51] as a result of the development of parametric instabilities.[41,42]

With respect to diagnosing the state of the compressed plasma core, the basic investigation methods here apparently are the method of x-ray spectroscopy[14,28,52,53] and of particle diagnostics.[11,12,54-58] In addition, it should be remembered that a quantitative study of neutron emission during heating of targets containing thermonuclear fuel (DD and DT mixtures) is the basic criterion which indicates the effectiveness of plasma heating and supports the validity of the laser-induced fusion concept.

Corresponding to the above-posed problems, the plasma diagnostics employed in the DELFIN facility can be divided into the following classes:

1. Optical diagnostics in the wavelength interval $\lambda = 0.35$ to 1.06 μm;
2. Plasma spectroscopy in high UV and soft x-ray spectra ($\lambda = 1$ to 10^3 Å);
3. Spectroscopy of the hard x-ray radiation ($\lambda < 1$ Å); and
4. Particle diagnostics.

The vacuum chamber and some elements of the diagnostics are shown schematically in Fig. 19.

Optical methods of investigation in the present work consist of high-speed, multiexposure, shadowgraph photography of the interaction process and interferometry of the plasma corona. The main aim of shadowgraph photography is the measurement of the fate of the energy absorbed in the plasma by the method based on the study of the dynamics of expanding shock waves generated by the plasma explosion in a background gas.[3,10,59,60] In addition, investigation of the initial stage of shock wave expansion, before the similarity regime corresponding to instantaneous point explosion,[61,62] allows estimation of hydrodynamic plasma parameters until the action of the laser beam is terminated. In this way can be carried out, for example, temperature measurements in the glowing plasma.[10,63] The optical scheme for the shadowgraph photography (see Fig. 19) consists of a ruby laser (oscillator, pulse length forming system, and an amplification stage) synchronized by means of an RLP with the high-energy neodymium laser, an optical-delay scheme, and a collecting-registering unit. The length of the illumination pulse is determined by the transmission

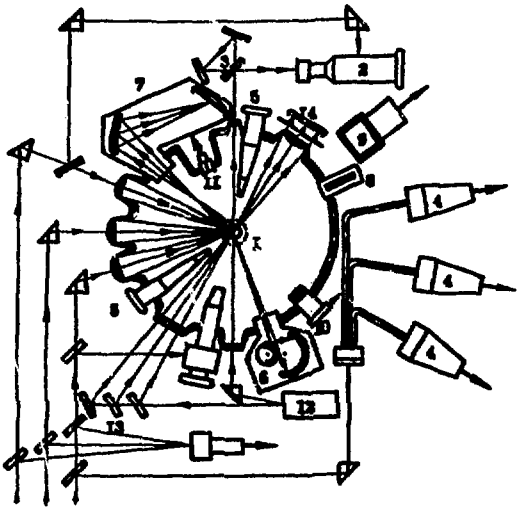

Fig. 19. Vacuum chamber and diagnostic instrumentation. 1-target, 2-image converter streak camera, 3-time-resolved interferometer, 4-scintillation neutron detectors, 5-pinhole camera, 6-x-ray spectrometer, 7-focusing x-ray spectrometer, 8-nuclear photoplate, 9-activation counter, 10-ion probe detector, 11-scintillation detector, 12-ruby laser, 13-optical delay system, 14-recorder of the shadowgraph.

window of the slicing cell which, in its construction, is analogous to the slicing Kerr cell in the neodymium laser and is $\tau \approx 0.5$ ns. The time intervals between frames can be changed in the range from 1 ns to 100 ns with the maximum delay of ~ 1 μs. In this way the system allows obtaining 19-frame shadowgraph UV images generated by the plasma glow in the background-gas atmosphere with time resolution of ~ 0.5 ns and spatial resolution $\sim 10^{-2}$ cm with the maximum frame repetition rate 1 GHz.

For the background the gas most often used is deuterium at a pressure $p \approx 5$ to 20 mm Hg.

The problem to be studied with high-speed interferometry of the laser plasma is the investigation of the time evolution of the density profile in the plasma "corona" in the interval 10^{18} cm^{-3} $< n_e < 10^{21}$ cm^{-3}. In the experiment utilized is the scheme of a time-resolved interferometer (see Fig. 19) with interferogram recording on an image converter streak camera. Spatial resolution of the interferometric system at the objective is ~20 μm and temporal ~ 0.1 ns. A light pulse from a ruby laser ($\lambda = 0.6943$ μm) and radiation at the second harmonic of the ruby laser emission are used as a light source for the interferometer. Length of the light source pulse $\tau = 25$ ns corresponds to the pulse length of the ruby laser before transmission through the pulse forming system. The EOP is synchronized with the subsequent process with the aid of an RLP triggered by radiation emission from the basic neodymium laser which is used for the formation of the scan pulse for EOP as in the work described in Ref. 64.

Simultaneously with the recording of interferograms with an image converter streak camera in this experiment utilized is high-speed frame interferometry[10,65] whose fundamental aim is the symmetry control of the plasma sphere which together with interest of its own (analysis of target heating symmetry) is very important from the point of view of correctness of reduction of interferograms recorded with the image converter streak camera.[64,66] In frame recording of the interferograms time resolution ~ 10^{-2} cm and time intervals between frames are 1.5 ns with number of frames equal to 7.

Analysis of the evolution of plasma density in the corona on the basis of interferometric measurements makes possible investigation of the mechanism of plasma ablation caused by the action of the reactive pressure pulse of the corona and estimation of the effectiveness of using target mass for its thermonuclear compression and heating. Comparison of the results of measurement with corresponding computations is very useful for the determination of the compression of dense plasma core.[3,10]

Spectroscopy in the regime of vacuum UV radiation ($\lambda = 50$-1000 Å) is used to investigate the line emission from plasma for diagnostics in the region $n_e \geq 10^{21}$ cm^{-3} and, together with interferometry in this range, makes it possible to investigate the time and spatial structures of the density profile. For diagnostic purposes a spectrograph is used with tangential incidence[67] (angles of incidence 86°, 88°, and 89°; radius of Rowland's circle 2000 mm) and diffraction (reflection) grating covered with gold and platinum.

The diagnostics of radiation emission from plasma in the regime of soft x-rays ($\lambda = 1$ to 10 Å) include means for recording line emission and light-gathering focusing spectrographs with concave crystals as in the schemes of Johann and Koshua.[69-71]

its purpose is to investigate temperature, plasma density, and plasma ionization state in different regions of the target.

For plasma diagnostics in the continuum x-ray emission with high spatial resolution (~ 10 μm at the objective) used are multichannel pinhole cameras[14,38,72] which record radiation on a special photoemulsion of the type UV-VR[73,74] after it is filtered through absorbers of different densities. This method is one of the ways to measure the magnitude of the compression in the dense target core[38] and allows, in principle, measurement of spatial distribution of density and temperature up to $n_e \approx 10^{25}$ cm^{-3}. Fundamental disadvantages of this methodology limiting its applications are the very low light-gathering power of the system (10^{-4} to 10^{-5}) and absence of time resolution.

To increase the light-gathering power and to improve spatial resolution of the diagnostics systems of the DELFIN facility a special mirror focusing system of crystal-analyzers bent at the P-order surfaces[75] is used allowing to increase the light gathering power to 10^{-2} to 10^{-3}. Development of this system made it possible to realize x-ray diagnostics of the laser plasma with time resolution ~ 0.6 ns. In it the photography of plasma in the light of specific x-rays can be accomplished both in the frame-imaging mode, using special lines of the optical delay and of the Pockels cell synchronized with the heating laser pulse with the aid of RLP, and in the image converter streak camera mode. A special fast scintillator[76] (luminescence time ~ 0.6 ns) is used in these methods to transform x-ray radiation into light.

Another x-ray spectroscopy method that allows laser plasma observations with time resolution is the recording of x-ray emission with the aid of coaxial photoelements of the type considered in Refs. 6 and 77. In our case a gold foil of 200-μm thickness is the cathode of the photoelement. Time resolution is ~ 0.7 ns.

Multichannel, high-sensitivity scintillation detectors are employed to record hard x-ray emission ($k\nu > 50$ keV), which contains information about fast (superthermal) electrons in the plasma. A plastic scintillator[78] (2% terphenyl + 0.02% ROROR in polystorol) with luminescence time of ~ 3 to 4 ns is used to transform x-ray emission into light and to obtain time resolution to the system.

Neutron measurements and ion probe detectors[56] are employed for particle diagnostics. Ion probe detectors are intended for measurement of spectral composition of ions emitted from the plasma in the ion energy range 1 to 100 keV. Neutron diagnostics include neutron time-of-flight measurements with neutron scintillation detectors[10,12] and quantitative measurements of neutron beams emitted from the plasma with nuclear photoemulsion[11] and activation counters (indium and silver). A special place here is occupied by the compression diagnostics from spectral composition and ratio of the quantity of DD neutrons to DT-type neutrons generated in the deuterium plasma.[12,58] Special scintillator detectors of very high sensitivity having time resolution of ~ 3 ns are used for this purpose; this allows sufficiently accurate measurements of the spectra and quantities of DD and DT neutrons at the level of 10^7 to 10^{10} neutrons per burst.

In concluding this work the authors consider it a pleasant duty to express their gratitude to Yu. M. Popov, D. V. Kovalevsky, and V. V. Nikitin for their interest; B. I. Belov, B. L. Vasyn, I. M. Dyvylkovsky, E. I. Merkulov, V. V. Sydorov, G. M. Starshynin, and R. S. Surgutskov for assistance in different planning stages; N. E. Bykovsky, M. V. Epifanov, M. P. Kalashnikov, B. V. Kozlov, S. A. Magnitskov, V. P. Osetrov, S. A. Pikuz, N. V. Pletnev, A. V. Rode, Yu. V. Senatsky, V. M. Solodkov, A. Ya. Faenov, A. A. Cygankov, and V. V. Chychmar for direct help in this work; and I. M. Buzhinskov, V. A. Grybkov, P. G. Kryukov, Yu. A. Merkulev, S. K. Mamonov, N. V. Morachevsky, and A. S. Shykanov for critical comments.

BIBLIOGRAPHY

1. N. G. Basov, and O. N. Krokhin, ZhETF 46, 171 (1964).

2. N. G. Basov, O. N. Krokhin, G. V. Sklizkov, A. I. Fedotov, and A. S. Shikanov, ZhETF 62, 203 (1972).

3. N. B. Basov, O. N. Krokhin, G. V. Sklizkov, and S. I. Fedotov, Proc. FIAN USSR 76, 146 (1974).

4. N. G. Basov, V. A. Gribkov, A. I. Isakov, N. V. Kalachev, O. N. Krokhin, B. V. Kruglov, V. Ya. Nikulin, O. G. Semenov, and G. V. Sklizkov, FIAN USSR Preprint No. 16 (1975).

5. M. J. Lubin, "Laser Fusion Feasibility Project," Annual report of the Laboratory for Laser Energetics (University of Rochester) (1973).

6. S. S. Sussman, W. Clements, G. Shaw, and P. Tanasovich (eds.), "Laser-Fusion Program Semi-annual Report, January-June 1973," Lawrence Livermore Laboratory report UCRL-40021-73-1 (1973).

7. F. Skoberne, "Laser Program at LASL," Los Alamos Scientific Laboratory report LA-5739-PR (1974).

8. D. Schirman, D. Billon, D. Cognard, J. Launspach, and C. Patou, Report at the VIII International Quantum Electronics Conference, San Francisco, CA (1974); Report at the V IAEA Conference on Plasma Physics and Controlled Nuclear Fusion Research, Tokyo, Japan (November 1974); Report at the VII Annual Meeting of the APS of Plasma Physics, St. Petersburgh, FL (1975).

9. N. G. Basov, O. N. Krokhin, and G. V. Sklizkov, Laser Interaction and Related Plasma Phenomena (Plenum Press, 2, 389 1972).

10. N. G. Basov, E. G. Gamaly, O. N. Krokhin, Yu. A. Mikhailov, G. V. Sklizkov, and S. I. Fedotov, FIAN USSR Preprint No. 15 (1974).

11. N. G. Basov, Yu. A. Ivanov, O. N. Krokhin, Yu. O. Mikhailov, G. V. Sklizkov, and S. I. Fedotov, ZhETF Lett. 15(10), 589 (1972).

12. N. G. Basov, Yu. A. Zakharenkov, O. N. Krokhin, Yu. A. Mikhailov, G. V. Sklizkov, and S. I. Fedotov, Quant. Elect. 1(9), 2069 (1974).

13. O. N. Krokhin, Yu. A. Mikhailov, V. V. Pustovalov, A. A. Rupasov, V. P. Silin, G. V. Sklizkov, and A. S. Shikanov, ZhETF Lett. 20(4), 239 (1974).

O. N. Krokhin, Yu. A. Mikhailov, V. V. Pustovalov, A. A. Rupasov, V. P. Silin, G. V. Sklizkov and A. S. Shikanov, ZhETF 69, 1(7), 207 (1975); FIAN USSR Preprint No. 22 (1975).

14. O. N. Krokhin, Yu. A. Mikhailov, A. A. Rupasov, G. V. Sklizkov, A. S. Shikanov, Yu. A. Zakharenkov, and N. N. Zorev, "Investigation of Spatial Density Distribution in Laser Plasma at Flux Densities of 10^{14}-10^{15} W/cm^2," Proc. 12th Intern. Conf. on Phenomena in Ionized Gases, Eindhoven (1975).

Yu. A. Zakharenkov, N. N. Zorev, O. N. Krokhin, Yu. A. Mikhailov, A. A. Rupasov, G. V. Sklizkov, and A. S. Shikanov, ZhETF Lett. 21(9), 557 (1976).

15. V. V. Alexandrov, E. P. Velikhov, A. G. Kaligin, N. G. Tselov, N. G. Kovalsky, V. V. Korobkin, P. P. Pashinin, M. I. Pergament, A. M. Prokhorov, and A. I. Yaroslavsky, "Investigation of Laser-Produced Plasma on 'Mishen' Devices," Proc. VI European Conf. on Controlled Fusion and Plasma Physics 2, 435 (1973).

I. N. Burdansky, N. G. Kovalsky, A. N. Kolomiisky, M. I. Pergament et al., Appl. Opt. 15, 7 (1976).

16. A. V. Dubovoy, V. D. Dyatlov, V. I. Kryzhanovsky, A. A. Mak, R. N. Medvedev, A. N. Popytaev, V. A. Serebryakov, V. N. Sysov, and A. D. Starykov, ZhTF XLIV(11), 2398 (1974). Preprint T-0135 NIIEFA (1974).

A. A. Gorokhov, V. D. Dyatlov, V. B. Ivanov, R. N. Medvedev, and A. D. Starykov, ZhETF Lett. 21(1), 62 (1975).

17. K. A. Brueckner, "Theory and Experiment in Laser Driven Fusion," Proc. VI European Conf. on Controlled Fusion and Plasma Physics 2, 259 (1973).

18. J. Nuckolls, L. Wood, G. Zimmerman, and A. Thiessen, Nature 239, 139 (1972).

19. Yu. V. Afanasyev, N. G. Basov, P. P. Volosevich, E. G. Gamaly, O. N. Krokhin, S. P. Kurdomov, E. I. Levanov, V. B. Rozanov, A. A. Samarsky, and A. N. Tikhonov, V Conf. on Plasma Physics and Controlled Thermonuclear Fusion, Tokyo, Japan (November 1974).

20. Yu. V. Afanasyev, N. G. Basov, P. P. Volosevich, E. G. Gamaly, O. N. Krokhin, S. P. Kurdymov, E. I. Levanov, V. B. Rozanov, A. A. Samarsky, and A. N. Tikhonov, ZhETF Lett. 21(2), 150 (1975).

21. J. Nuckolls, J. Lindl, W. Mead, A. Thiessen, L. Wood, and G. Zimmerman, "Laser Driven Implosion of Hollow Pellets," Report IAEA-CN-33/F 5-4 (November 1974).

22. G. Charatis, J. Downward, R. Goforth, B. Guecott, T. Henderson, S. Hildum, R. Johnson, K. Moncur, T. Leonard, F. Heyer, S. Segall, L. Siebert, D. Solomon, and G. Thomas, "Experimental Study of Laser Driven Compression of Spherical Glass Shells," V IAEA Conf. on Plasma Physics and Controlled Nuclear Fusion Research, Tokyo, Japan (November 1974).

23. G. S. Fraley, W. P. Gula, D. B. Henderson, R. L. McCrory, R. C. Malone, R. J. Mason, and R. L. Morse, "Implosion Stability and Burn of Multishell Fusion Pellets," Report IAEA-CN-33/I F5-5 (November 1974).

24. E. G. Gamaly, A. I. Isakov, Yu. A. Merkulev, A. I. Nikitenko, E. R. Rychkov, and G. V. Sklizkov, Quant. Elect. 2(5), 1043 (1975).

25. R. J. Mason, "Performance of Structured Laser Fusion Pellets," Los Alamos Scientific Laboratory Preprint LA-UR-75-260 (1975).

26. S. I. Anisimov, M. F. Ivanov, P. P. Pashinin, and A. M. Prokhorov, ZhETF Lett. 22(6), 343 (1975).

27. N. G. Basov, A. E. Danilov, O. N. Krokhin, Yu. A. Mikhailov, G. V. Sklizkov, and S. I. Fedotov, FIAN, USSR Preprint No. 30 (1976).

28. N. G. Basov, O. N. Krokhin, G. V. Sklizkov, and S. I. Fedotov, FIAN USSR Preprint No. 51 (1974).

29. N. E. Bykovsky, S. M. Zakharov, N. V. Pletnev, Yu. V. Senatsky, and S. I. Fedotov, FIAN USSR Preprint No. 137 (1975).

30. B. R. Belostotsky, Yu. V. Ljubavsky, and V. M. Ovchinnikov, "Fundamentals of Laser Technology," Soviet Radio, Moscow (1972).

31. V. A. Gribkov, G. V. Sklizkov, S. I. Fedotov, and A. S. Shikanov, PTE 4, 213 (1971).

32. E. R. Mustel, and V. N. Parygin, Methods for Modulation and Analysis of Light (Nauka, Moscow 1970).

33. N. G. Basov, O. N. Krokhin, A. A. Rupasov, G. V. Sklizkov, and S. I. Fedotov, FIAN USSR Preprint No. 47 (1973).

34. C. E. Thomas, Appl. Opt. 14(6), 1267.

C. E. Thomas, Laser Focus 6, 49 (1975).

35. J. DeMetz, L'Onde Electrique 50(7), 572 (1970).

36. A. A. Rupasov, G. V. Sklizkov, V. P. Tsapenko, and A. S. Shikanov, ZhETF 65, 1898 (1973). A. A. Rupasov, V. P. Tsapenko, and A. S. Shikanov, FIAN USSR Preprint No. 94 (1972).

37. N. G. Basov, O. N. Krokhin, V. V. Pustovalov, A. A. Rupasov, V. P. Silin, G. V. Sklizkov, V. T. Tikhonchuk, and A. S. Shikanov, ZhETF 67, 118 (1974); FIAN USSR Preprint No. 17 (1974).

38. P. M. Campbell, G. Charatis, and G. R. Montry, Phys. Rev. Lett. 45(2), 73 (1974).

K. A. Brueckner, P. M. Campbell, and R. A. Grandey, Nucl. Fusion 15, 471 (1975).

B. R. Guscott, G. Charatis, J. S. Hildum, R. R. Johnson, F. J. Mayer, N. K. Moncur, D. E. Solomon, and C. E. Thomas, "KMS Fusion High Powered Laser for Fusion Experiments, Its Performance and Experimental Application," VII European Conf. on Controlled Fusion and Plasma Physics, Lausanne, Switzerland (1975).

39. K. G. Whitney and J. Davis, Appl. Phys. Lett. 24(10), 509 (1974).

40. P. J. Mallozzi, H. M. Epstein, R. G. Jung, D. C. Applebaum, B. P. Fairand, and W. J. Gallagher, "X-ray Emission from Laser Generated Plasmas, Final Report, Vol. II," Battelle Columbus Laboratories (1972).

P. J. Mallozzi, H. M. Epstein, R. G. Jung, D. C. Applebaum, B. P. Fairand, W. J. Gallagher, and B. E. Campbell, Bull. APS II, 12(97, 923 (1974).

41. V. P. Silin, Parametric Influence of High Intensity Radiation on Plasma (Nauka, Moscow 1973).

42. V. V. Pustovalov, V. P. Silin, and V. T. Tykhonchuk, ZhETF Lett. 17(2), 120 (1973).

43. K. Eidman and R. Sigel, "Investigation of the Fast Electrons in a Laser Produced Plasma by X-ray Measurements," Proc. VI European Conf. on Controlled Fusion and Plasma Physics, 435 (1973).

44. R. P. Godwin, J. F. Kephart, and G. H. McCall, Bull. Am. Phys. Soc. 971 (1972).

45. V. A. Bojko, Yu. A. Drozhbyn, S. M. Zakharov, O. N. Krokhin, V. Ya. Nikulin, S. O. Pikuz, G. V. Sklizkov, A. Ya. Faenov, Yu. V. Chertov, and V. A. Yakovlev, FIAN USSR Preprint No. 77 (1973).

46. R. Zigel, C. Vitkovsky, Kh. Baumkhakker, K. Vyukhl, K. Aidman, Kh. Khora, Kh. Menike, P. Mulcer, D. Pfirsch, and Kh. Zaitsman, Quant. Elect., N. G. Basov, ed. 2(8), 37 (1972).

47. L. M. Goldman, J. Soures, and M. J. Lubin, Nucl. Fus. 13, 839 (1973).

48. N. G. Basov, V. A. Bojko, S. M. Zakharov, O. N. Krokhin, Yu. A. Mikhailov, G. V. Sklizkov, and S. I. Fedotov, ZhETF Lett. 18, 314 (1973).

49. G. H. McCall, F. Young, A. W. Ehler, J. F. Kephart, and R. P. Godwin, Phys. Rev. Lett. 30, 116 (1973).

50. G. H. McCall, "Fast Ion Production in Laser Produced Plasmas," Proc. of Fuji Seminar on Laser Interaction with Plasma, 57 (1975).

51. V. P. Silin, ZhETF Lett. 21(6), 333 (1975).

52. V. A. Bojko, S. A. Pikuz, and A. Ya. Faenov, Quant. Elect. 2(6), 1216 (1975).

53. E. V. Anglicky, V. A. Bojko, A. V. Vinogradov, and E. A. Yukov, Quant. Elect. 1, 579 (1974).

54. O. N. Krokhin, F. A. Nikolaev, and G. V. Sklizkov, ZhETF Lett. 19(6), 389 (1974).

55. V. W. Slivinsky, H. G. Ahlstrom, K. G. Tirsell, J. Larsen, S. Glaros, G. Zimmerman, and H. Shay, Lawrence Livermore Laboratory preprint UCRL-76938 (1975).

56. G. Charatis, J. Downward, R. Goforth, B. Guscott, T. Henderson, S. Hildum, R. Johnson, K. Moncur, T. Leonard, F. Mayer, S. Segall, L. Siebert, D. Solomon, and C. Thomas, "Experimental Study of Laser Driven Compression of Spherical Glass Shells," Proc. of Fuji Seminar on Laser Interaction with Plasma, 73 (1975).

57. A. W. Ehler, J. Appl. Phys. 46(6), 2464 (1975).

58. E. G. Gamaly, S. Yu. Guskov, O. N. Krokhin, and V. B. Rozanov, ZhETF Lett. 21(2), 156 (1975).

59. V. Ya. Goldin, and B. N. Chetvertushkin, ZhETF 68(5), 1768 (1975).

60. T. A. Leonard, and F. J. Mayer, J. Appl. Phys. 46(8), 3562 (1975).

61. Ya. B. Zeldovich, and Yu. P. Raizer, The Physics of Shock Waves and High Temperature Phenomena (Nauka, Moscow 1966).

62. V. P. Korobejnikov, N. A. Molnikov, and E. V. Ryazanov, Theory of Point Explosion (GIFML, Moscow 1961).

63. G. V. Sklizkov, Generation and Investigation of High-Temperature Superdense Plasma with Laser Heating (Dissertation) (FIAN, Moscow, 1973).

64. V. M. Groznov, A. A. Erokhin, Yu. A. Zakharenkov N. N. Zorev, N. A. Konoplev, O. N. Krokhin, G. V. Sklizkov, S. I. Fedotov, and A. S. Shikanov, FIAN USSR Preprint No. 50 (1975).

65. G. V. Sklizkov, Laser Handbook, 2, 1545 (North-Holland Publ. Co. 1972).

66. Yu. A. Zakharenkov, N. N. Zorev, A. A. Kologrivov, N. A. Konoplev, G. V. Sklizkov, and S. I. Fedotov, FIAN USSR Preprint No. 121 (1973).

67. A. H. Gabriel, J. R. Swain, and W. A. Waller, J. Scient. Inst. 42, 94 (1965).

A. H. Gabriel, G. B. F. Niblett, and N. J. Peacock, J. Quant. Spect. Rad. Trans. 2, 491 (1963).

68. E. V. Anglicky, and V. A. Bojko, FIAN USSR Preprint No. 79 (1974).

69. Yu. A. Mikhailov, G. A. Pikuz, A. Ya. Faenov, S. I. Fedotov, PTF (1976).

70. Yu. A. Mikhailov, S. A. Pikuz, G. V. Sklizkov, A. Ya. Faenov, and S. I. Fedotov, FIAN USSR Preprint No. 21 (1976).

71. G. V. Peregudov, E. N. Ragozin, and V. A. Chirkov, Quant. Elect. 2(8), 1844 (1975).

72. M. H. Key, K. Eidmann, C. Dorn, and R. Sigel, Phys. Lett. 48A(2), 121 (1974).

73. A. A. Kologrivov, Yu. A. Mikhailov, G. V. Sklizkov, S. I. Fedotov, A. S. Shikanov, and M. R. Shpolsky, Quant. Elect. 2(10), 2223 (1975).

74. E. V. Anglicky, V. A. Bojko, T. N. Kalinkin, A. N. Oshurkov, S. A. Pikuz, V. M. Uvarov, A. Ya. Faenov, and M. R. Shpolsky, PTE 4, 913 (1975).

75. L. M. Belaev, A. B. Gilbarg, Yu. A. Mikhailov, S. A. Pikuz, G. V. Sklizkov, A. Ya. Faenov, and S. I. Fedotov, Quant. Elect. 8, 3 (1976).

76. S. F. Kilin, K. A. Kovirzin, Yu. P. Kushakevich, I. M. Rozman, and V. M. Shonin, "Fast Acting Plastic Scintillators," XXII All Union Symposium on Luminescence.

Yu. S. Kasianov, V. V. Korobkin, P. P. Pashinin, A. M. Prokhorov, V. K. Chevokin, and M. Ya. Shchelev, ZhETF Lett. 20(11), 719 (1974).

77. M. H. Key, K. Eidmann, C. Dorn, and R. Sigel, Appl. Phys. Lett. 25(6), 335 (1974).

78. A. S. Isajev, M. N. Medvedev, and V. I. Prokhorov, "Scintillators and Scintillator Materials," Conf. Proc., Kharkov (1963).

LIMITS OF POSSIBILITIES FOR HEATING SPHERICAL TARGETS WITH LASER RADIATION*

In the majority of investigations of laser-initiated thermonuclear fusion (LTS) principal attention is devoted to the study of physical processes occuring in thermonuclear plasma[8-11,22-26] during heating with high-energy light radiation and to the achievement of physically useful thermonuclear energy yield.[12-16] In these studies it is assumed as a rule that the laser beam parameters are such as to assure sufficient energy deposition in the absorption zone and the question of the possibility of attaining such required regime of (laser) facility operation is not considered.

To assess the prospects of one or another approach to LTS, it is necessary to analyze the possibilities for attaining a parameter overlap between the laser-target system and the laser beam radiation. In the existing literature the problem of attainable limits in the concentration of laser radiation on the target surface has not been considered. Estimates obtained in Ref. 3 were based on idealized values of radiation parameters, which can be barely realized with great effort in the most simple single lasers. In multibeam laser systems used for spherical heating of plasma, it is not possible to achieve such careful adjustments and correlations of the temporal and spatial structure of radiation in all the beams; this leads to significant departures of radiation parameters from their ideal values and thus significantly limits the range of applicability of different LTS concepts.

We will now examine the question of attainable limits in spherical irradiation of plasma with high-energy laser pulses, taking into account the realistically attainable values of radiation parameters.[17]

The limiting value of the brightness B_{pr} of laser radiation with total energy E_L and a total output cross-section area of the active medium, S, for the pulse length τ is related to the intensity $\varepsilon_{pr} = E_L/S$, and beam divergence α by

$$B_{pr} = \varepsilon_{pr}/(\pi\alpha^2\tau) . \qquad (1)$$

On the other hand, using the Lagrange-Helmholtz theorem, the laser brightness B can be expressed in terms of parameters describing radiation at the target of radius r_o in the following form:

$$B = E_L/(16\pi^2\xi\eta\tau r^2) . \qquad (2)$$

In expression (2) account is taken of the fact that the full solid angle of the radiation convergence onto the target from the last component of the focusing optics, which has a transmission coefficient ξ and occupies a sphere of radius equal to the focal length with a fill coefficient η, equals $4\pi\eta$. Obviously, the inequality $B \leq B_{pr}$ is a condition for an effective plasma heating.

We will now make a few comments about the quantities α and ε_{pr}. The divergence of the laser radiation at the output is determined by the quality of the optical medium (optical inhomogeneity, double refraction, internal flaws, etc.) and errors in surface finish of optical elements (deviations of shapes of working surfaces from prescriptions, imperfect alignment, wedge effects, polishing, etc.). An increase in laser energy is accompanied by an increase of the optical path in the active medium, L, and an increase of the number of optical surfaces, N_p, which lead to worsening laser beam divergence.

Concerning the volume quality of the optical medium, it is appropriate to consider that the main reason for the increasing angular beam divergence is the optical distortion of active laser elements at the time of optical pumping[27,28] caused by the nonuniform heating of the rods, and connected with it, thermal distortions of the rods and fluctuations in the refraction index n. Note that when the distortion is sufficiently symmetric, the distortion effect of the propagating wave front becomes equivalent to

*Translator's note: This section is translated from FIAN USSR Preprint No. 151 (1976), "High Energy Laser Thermonuclear Facility 'Delfin'" by N. G. Basov, O. N. Krokhin, Yu. A. Mikhailov, G. V. Sklizkov, S. I. Fedotov. Preprint No. 151 is a less detailed description of the DELFIN facility than the one provided in Preprint No. 74 and translated in full; however, material in this section is not contained in Preprint No. 74, and therefore is appended here for the sake of completeness.

the action of some positive or negative lens[28,29] which can be compensated for, to greater or lesser degree, with the addition of supplementary optical elements at the output end.[30]

On the other hand, small fluctuations in the surface finish of the optical elements capable of increasing beam divergence substantially cannot be compensated for, and their effect on the beam divergence is determined only by the number of surfaces and the quality of finish.

To estimate the effects of the optical surface imperfections at some reference distance D leading to wavefront deformation and to beam divergence, one can use the concept of an "effective lens" and write

$$\alpha = \operatorname{arctg}\left[\frac{4\Delta_o}{n_1 D}(n_2 - n_1)\sqrt{N_p}\right], \qquad (3)$$

where n_1 and n_2 are indices of refraction of optical media separated by a surface with imperfections Δ_o and the factor $N_p^{1/2}$ accounts in the mean square sense for the cumulative effect of individual imperfections considered as random variations. To obtain numerical estimates, Δ_o can be taken to be equal to the mean surface deviation of the optical element from the sphere or the plane, which in optics is usually expressed in terms of the number of interference rings or fringes, ΔN. In accordance with tolerances for reflecting surfaces of mirror-prism systems,[31] we choose $\Delta N = 0.5$ (high-accuracy group) which corresponds to limits attainable in routine finishing of a large number of optical surfaces in the laser system.

For a multibeam laser system of the kind described in Refs. 2, 3, and 5 containing n_k stages with number of surfaces in the stage $m = N_p/n_k$ and the amplification coefficient for the stage k the overall number of surfaces in each beam depends on the total system output energy in the following way:

$$N_p \simeq \frac{m}{\ell n k}\ell n\,(E_p/\varepsilon_{pr}S_o), \qquad (4)$$

where S_c -cross-section area of the light beam at the entrance to the first amplification stage. It should be noted that the high-energy amplification stages of the DELFIN facility are constructed in accordance with such principle and satisfy estimate (4).

In the following analysis of beam divergence considered are lasers with rod (m = 10) and disk (m = 34) amplifiers. In the analysis of the system with rod amplifiers, it is assumed that active elements have the same length $L = (\ell n\, k)/\kappa = 560$ mm (κ - gain coefficient per unit length) and diameter of 45 mm, which corresponds to maximum allowable output energy of ~ 50 J at the exit from the first amplification stage in a nanosecond interval. In the computations the value k = 3 is used, which is characteristic for active elements with the above dimensions made of GLS-1 glass in the saturated gain regime (flux density $q \gtrsim 1$ GW/cm^2). The value m = 10 is chosen on the basis of experimental data[2,3] and consistently with the construction scheme of the amplification stages of the DELFIN facility.

For the laser system of the type described in Ref. 7 with disk amplifiers of active thickness ℓ and aperture $D_o = 2(S_D/\pi)^{1/2}$, the number of optical surfaces (N_{PD}) in the channel increases relative to the rod system (N_{PS}) approximately as

$$\frac{N_{pD}}{N_{ps}} \simeq \left(1 + \frac{2\,\ell n\, k}{\kappa \ell m}\right)\ell n\left(\frac{E_L}{\varepsilon_{pr}S_D}\right)\Big/\ell n\left(\frac{E_L}{\varepsilon_{pr}S_c}\right). \qquad (5)$$

It should be noted that with increasing apertures of optical elements the imperfections in their manufacture increase as also do distortion of the optical elements caused by their own weights. The result is a 2 to 3 times worse beam divergence for disk systems than for rod systems.

With respect to the allowable beam intensity in the optical medium, we note that its magnitude depends essentially on the parameters of the amplified pulse and, most of all, on its length that determines the relevant mechanism, which limits the attainable flux density in the medium. Thus for very short pulses with length $\tau \approx 10^{-12}$ to 10^{-10} s the limiting mechanism is self-focusing of laser radiation, and for $\tau \approx 10^{-8}$ to 10^{-7} s, the mechanism is disturbance of optical surfaces. Experimental data obtained for Nd-glass in different installations[32] suggest the following expression to approximate the dependence of $\varepsilon_{pr}(\tau)$ in the interval $\tau \approx 10^{-11}$ to 10^{-7} s:

$$\varepsilon_{pr} \simeq \varepsilon_o \tau^{*1/2}, \qquad (6)$$

where $[\varepsilon_{pr}]$ = J/cm^2, ε_o = 3 J/cm^2, τ^* = nondimensional time ($\tau^* = \tau/\tau_o$; $\tau_o = 10^{-9}$ s). Substituting expressions for α, N_p, and ε_{pr} into Eqs. (1) and (2), the inequality $B \leq B_{pr}$ can be rewritten in the form

$$r \geq r_1$$

$$\cong \frac{\Delta_o (n_2 - n_1) E_L^{1/2} \ell n^{1/2} (E_L/\varepsilon_o \tau^{*1/2} S_o)^{m/\ell n\, k}}{n_1 D \tau^{*1/4} (\pi \eta \varepsilon_o \xi)^{1/2}}, \text{ cm.} \tag{7}$$

The expression thus obtained imposes a lower bound on the radius of the target, which can be heated by a laser beam without losses connected with the impossibility to concentrate light energy in very small volumes with the existing optics.

On the other hand, effective heating of plasma to temperatures which ensure specific energy per unit mass ε with effectiveness ζ of energy conversion from laser radiation into thermal, and with the coefficient γ giving the fraction of volume of (4/3) r^3 occupied by the target matter of density, ρ_o is possible only if the condition

$$r \leq r_2 = \left(\frac{3 E_L \zeta}{4\pi \rho_o \gamma \varepsilon}\right)^{1/3} \tag{8}$$

is satisfied; this is an upper bound on the allowable target radius.

Families of curves, $r_{1,2}(\tilde{E}_L)$ delineating admissable ranges of thermonuclear target sizes, which can be heated in laser facilities with rod elements with m = 10 and with energy up to 5×10^7 J, are given in Fig. 1. In Fig. 1 and in what follows $\tilde{E}_L$ is the normalized laser energy $\tilde{E}_L = E_L/\varepsilon_{pr} S_o$ ($S_o \approx 16$ cm^2, corresponding to a light beam of diameter 45 mm, light intensity is taken to be ε_{pr} = 3 J/cm^2, and pulse length $\tau \approx 1$ ns). Dashed curves correspond to bounds on the radius of glass (ρ_o = 2.5 g/cm^3) microballoons ($r \leq r_2$). Used as a parameter here is the coefficient γ that varies between the limits of 0.2 and 0.005, which for r = 500 μm corresponds to wall thicknesses in the range 1 to 30 μm. Dash-dot curve corresponds to $r_2(\tilde{E}_L)$ for solid target (γ = 1) of frozen DT ($\rho_o \approx 0.25$ g/cm^3). The parameter for solid curves, which define limit of energy concentration in the target ($r \geq r_1$), is the

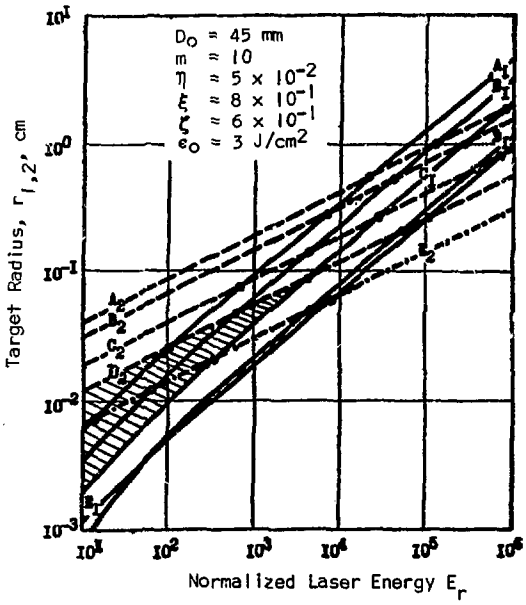

Fig. 1. Dependence of limiting values, r_1 (——) and r_2 (---), of target radius on laser energy for the system with active elements in the form of 45-mm-diam rods. For ΔN = 0.5; A_1 is τ = 0.5 ns, B_1 is τ = 2 ns, C_1 is τ = 10 ns, D_1 is $\tau = 10^2$ ns. E_1 is τ = 0.5 ns with ΔN = 0.1. With ρ_o = 2.5 g/cm^3 and $\varepsilon = 10^8$ J/g, A_2 is $\gamma = 5 \times 10^{-3}$, B_2 is $\gamma = 10^{-2}$, C_2 is $\gamma = 5 \times 10^{-2}$, and D_2 is $\gamma = 2 \times 10^{-1}$. With ρ_o = 0.25 g/cm^3 and $\varepsilon = 10^9$ J/g, E_2 is $\gamma = 10^0$. Cross-hatched region is the range of admissable values of target radius in the case "C_1 - D_2".

pulse length varying from τ = 0.5 ns to τ = 100 ns. From Fig. 1 it is clear that with increasing energy of the laser system, the range of allowable values of r narrows and there exists a certain limiting value E_L^{pr} determined by the transcendental equation

$$\frac{\Delta_o}{D} (n_2 - n_1) \ell n^{1/2} \left(\frac{E_L^{pr}}{\varepsilon_o \tau^{*1/2} S_o}\right)^{m/\ell n\, k}$$

$$= \frac{n_1}{(E_L^{pr})^{1/6}} \left(\frac{3\zeta\sqrt{\pi}}{4}\right)^{1/3} (\eta \xi \varepsilon_o)^{1/2} \frac{\tau^{*1/4}}{(\rho_o \gamma \varepsilon)^{1/3}}. \tag{9}$$

Thus obtained expression makes it possible to analyze the influence of different factors on the magnitude of achievable energy. For example, for a disk laser system with m = 34, ℓ = 50 mm and D_o = 300 mm, the

ultimately achievable energy during heating of microballoon targets ($\gamma = 5 \times 10^{-3}$) with a laser pulse $\tau = 2$-ns long is $E_L^{pr} \approx 6 \times 10^5$ J, which, by comparison, is an order of magnitude lower than the energy achievable in the case when active rod elements are used with m = 10; D_o = 45 mm (see Fig. 2). Figure 2 also illustrates advantages of microballoon-type targets with respect to the attainment of higher values of E_L^{pr}: decreasing γ from 2×10^{-1} to 5×10^{-3}, for example, allows E_L to increase 200-fold.

In rod laser systems it appears expedient to increase rod diameters while keeping length of active elements constant. However, not much gain can be made along this direction because, first of all, the rod pumping effectiveness decreases drastically with increasing diameter above 60 mm (for existing types of glass, e.g. GLS-1), and second, the dependence of $\tilde{E}_L^{pr}$ on diameter is not sufficiently strong. Thus for a fourfold increase in the cross-sectional area of the active element the (ultimately) attainable laser energy only doubles.

It appears most fruitful to utilize optimal target constructions to increase the ultimately attainable energy. As it turns out, from the point of view of achieving limiting values of target heating, microballoon targets possess a number of advantages in comparison with solid spherical targets. We will consider them in more detail. In Fig. 3 are shown the dependencies of $\tilde{E}_L^{pr}$ on the length of the laser pulse, on the target wall thickness δ related to the target fill γ by the relations $\gamma = 3(\delta/r)[1 - (\delta/r) + (\delta^2/3r^2)]$, and on the initial target density ρ_o. Continuous curves correspond to the dependence $\tilde{E}_L^{pr}(\tau)$ for disk and rod systems, dotted curve gives $\tilde{E}_L^{pr}(\rho_o)$, and dash-dot curves $\approx E_L^{pr}(\tau)$ for active rod elements. These results (see also Fig. 1) clearly illustrate the hopelessness of the approach to laser-initiated fusion problems within the framework of a model based on the isentropic compression of a homogeneous target.[12] Utilization of nonhomogeneous

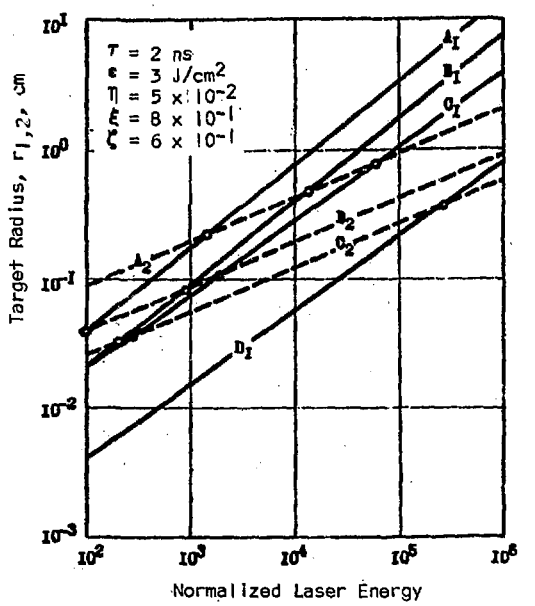

Fig. 2. Comparison of dependencies of limiting values r_1 (—) and r_2 (---) of target radius on laser energy for facilities with rod (m = 10; D_o = 45 mm) and disc (m = 34, D_o = 300 mm) active elements. A_1 is m = 34, D_o = 300 mm, ΔN = 1; B_1 is m = 34, D_o = 300 mm, ΔN = 0.5; C_1 is m = 10, D_o = 45 mm, ΔN = 0.5; D_1 is m = 10, D_o = 45 mm, ΔN = 0.1; A_2 is $\gamma = 5 \times 10^{-3}$; B_2 is $\gamma = 5 \times 10^{-2}$; and C_2 is $\gamma = 2 \times 10^{-1}$.

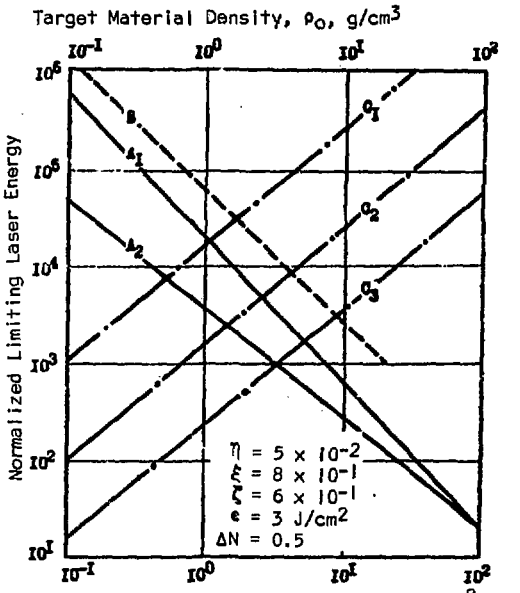

Fig. 3. Dependence of limiting laser energy on target fill coefficient γ (——), target material density ρ_o (---), and laser pulse length τ (— . —). A_1 is m = 10, D_o = 45 mm, τ = 1 ns; A_2 is m = 34, D_o = 300 mm, τ = 1 ns; B is m = 10, D_o = 45 mm, τ = 1 ns, $\gamma = 10^{-2}$. With m = 10 and D_o = 45 mm, C_1 is $\gamma = 10^{-2}$, C_2 is $\gamma = 5 \times 10^{-2}$, and C_3 is $\gamma = 2 \times 10^{-1}$.

microballoon targets[13-16] allows a substantial advance along the road toward experimental realization of laser-initiated fusion. Also, in this case the situation may be improved by simultaneously changing several variables present in Eq. (9) to assume more favorable values. In the case of microballoon targets the pulse length may reach 1 to 10^2 ns; parameter γ, depending on target construction can, in principle, be made sufficiently small, e.g., 10^{-1} to 10^{-3}. In addition one can count on certain reduction in the required internal plasma energy because of optimal distribution of density and temperature during final compression stage. In this way, in the construction of high-energy laser systems for the laser-induced fusion it becomes necessary to increase τ and to decrease γ and ρ_0 which favors targets with sufficiently thin and light spherical walls.

In concluding this section, we remark about the specific characteristics of laser systems with CO_2 gas for active medium. Except for the mechanisms of radiation absorption and heat conduction in the target which we will not consider, considerations similar to the above presented can be extended to CO_2 lasers. However, because of the fact that the allowable beam intensity in the optical medium used in CO_2 lasers is several times lower[33] than in Nd-glass lasers, the requirements on the parameter γ are correspondingly more restrictive.

BIBLIOGRAPHY*

2. N. G. Basov, O. N. Krokhin, G. V. Sklizkov, S. I. Fedotov, A. S. Shikanov, ZhETF 62, 203 (1972).

3. N. G. Basov, O. N. Krokhin, G. V. Sklizkov, S. I. Sklizkov, S. I. Fedotov; Proc. FIAN USSR 76, 146 (1974).

7. S. S. Sussman, W. Clements, G. Shaw, P. Tanasovich (eds), "Laser Fusion Program Semiannual Report, January-June 1973," Lawrence Livermore Laboratory report UCRL-50021-73-1 (1973).

8. N. G. Basov, E. G. Gamaly, O. W. Krokhin, Yu. A. Mikhailov, G. V. Sklizkov, S. I. Fedotov, Laser Interaction and Related Plasma Phenomena, (Plenum Press, 28, 553, 1974).

9. N. G. Basov, Yu. A. Zakharenkov, O. N. Krokhin, Yu. A. Mikhailov, G. V. Sklizkov, S. I. Fedotov, Quant. Elect. 1(9), 2096 (1974).

10. O. N. Krokhin, Yu. A. Mikhailov, V. V. Pustovalov, A. A. Rupasov, V. P. Silin, G. V. Sklizkov, A. S. Shikanov, ZhETF Lett. 20(4), 239 (1974); ZhETF 69 1 (7), 206 (1975).

11. O. N. Krokhin, Yu. A. Mikhailov, A. A. Rupasov, G. V. Sklizkov, A. S. Shikanov, Yu. A. Zakharenkov, N. N. Zorev, Proc. 12 International Conf. on Phenomena in Ionized Gases, Eindhoven, 349 (1975).

    Yu. A. Zakharenkov, N. N. Zorev, O. N. Krokhin, Yu. A. Mikhailov, A. A. Rupasov, G. V. Sklizkov, A. S. Shikanov, ZhETF Lett. 21(9), 557 (1975); ZhETF 70(2), 547 (1976).

12. J. Nuckolls, L. Wood, G. Zimmerman, A. Thiessen, Nature 239, 139 (1972).

13. Yu. V. Afanasiev, N. G. Basov, P. P. Volosevich, E. G. Gamaly, O. N. Krokhin, S. P. Kurdimov, E. I. Levanov, V. B. Rozanov, A. A. Samarskij, A. M. Tikhonov, ZhETF Lett. 21(2), 150 (1975).

15. G. Charatis, J. Downward, R. Goforth, B. Guscott, T. Henderson, S. Hildum, R. Johnson, K. Moncur, T. Leonard, F. Hayer, S. Segall, L. Siebert, D. Solomon, G. Thomas, "Experimental Study of Laser Driven Compression of Spherical Glass Shells," IAEA Conf. on Plasma Physics and Controlled Nuclear Fusion Research, Tokyo, Japan (November 11-15, 1974).

16. G. S. Fraley, W. P. Gula, D. B. Henderson, R. L. McCrory, R. C. Malone, E. J. Mason, R. L. Morse, "Implosion, Stability and Burn of Multishell Fusion Pellets," report IAEA-CN-33/1 F5-5 (1974).

17. O. N. Krokhin, Yu. A. Mikhailov, G. V. Sklizkov, S. I. Fedotov, Quant. Elect. 3(3), 636 (1976).

22. A. A. Rupasov, G. V. Sklizkov, V. P. Tsapenko, A. S. Shikanov, ZhETF 65, 1898 (1973); FIAN USSR Preprint No. 53 (1973).

    N. G. Basov, O. N. Krokhin, V. V. Pustovalov, A. A. Rupasov, V. P. Silin, G. V. Sklizkov, V. T. Tikhonchuk, A. S. Shikanov, ZhETF 67, 118 (1974); FIAN USSR Preprint No. 17 (1974).

23. P. M. Campbell, G. Charatis, G. R. Montry, Phys. Rev. Lett. 34(2), 74 (1974).

24. K. A. Brueckner, P. M. Campbell, R. A. Grandey, Nucl. Fus. 15, 471 (1975).

25. B. R. Guscott, G. Charatis, J. S. Hildum, R. R. Johnson, P. J. Mayer, N. K. Moncur, D. E. Solomon, C. E. Thomas, "KMS Fusion High Powered Laser for Fusion Experiments, its Performance and Experimental Application," VII European Conf. on Controlled Fusion and Plasma Physics, Lausanne, Switzerland (1975).

26. N. G. Basov, A. A. Kologrivov, O. N. Krokhin, A. A. Rupasov, G. V. Sklizkov, A. S. Shikanov, ZhETF Lett. 23, 474 (1976).

*Original numbering is maintained, however only references called out in this section are listed.

27. A. P. Veduta, A. M. Leontovich, V. N. Smorchkov, ZhETF 48, 87 (1965).

28. E. P. Riedel, G. D. Baldurin, Journ. Appl. Phys. 38(7), 2720 (1967); 38(7), 2726 (1967).

29. J. W. Bradford, R. C. Eckardt, Appl. Opt. 1(12), 2418 (1968).

30. W. F. Hafen, J. Appl. Phys. 40, 2 (1969).

31. M. Ya. Kruger et al., "Optico-Mechanical Apparatus Construction Handbook," Machine Design (1967).

32. A. J. Glass, A. H. Guenther (eds.), "Laser Induced Damage in Optical Materials: 1973," NBS Special Publication 387 (1974).

33. A. J. Glass, A. H. Guenther (eds.), "Laser Induced Damage in Optical Materials: 1974," NBS Special Publication 414 (1975).